

# Quantum field theory and the Standard Model

*W. Hollik*

Max Planck Institut für Physik, Munich, Germany

## Abstract

In this lecture we discuss the basic ingredients for gauge invariant quantum field theories. We give an introduction to the elements of quantum field theory, to the construction of the basic Lagrangian for a general gauge theory, and proceed with the formulation of QCD and the electroweak Standard Model with electroweak symmetry breaking via the Higgs mechanism. The phenomenology of  $W$  and  $Z$  bosons is discussed and implications for the Higgs boson are derived from comparison with experimental precision data.

## 1 Introduction

Relativistic quantum field theory is the adequate theoretical framework to formulate the commonly accepted theory of the fundamental interactions, the Standard Model of the strong and the electroweak interactions [1–4]. The Standard Model summarizes our present knowledge of the basic constituents of matter and their interactions. It is a gauge invariant quantum field theory based on the symmetry group  $SU(3) \times SU(2) \times U(1)$ , with the colour group  $SU(3)$  for the strong interaction and with  $SU(2) \times U(1)$  for the electroweak interaction spontaneously broken by the Higgs mechanism. The renormalizability of this class of theories allows us to make precise predictions for measurable quantities also in higher orders of the perturbative expansion, in terms of a few input parameters. The higher-order terms contain the self-coupling of the vector bosons as well as their interactions with the Higgs field and the top quark, even for processes at lower energies involving only light fermions. Assuming the validity of the Standard Model, the presence of the top quark and the Higgs boson in the loop contributions to electroweak observables allows us to obtain indirect significant bounds on their masses from precision measurements of these observables. The only unknown quantity at present is the Higgs boson. Its mass is getting more and more constrained by a comparison of the Standard Model predictions with the experimental data, preparing the ground for a crucial test at the LHC.

In these lectures we give an introduction to the basic elements of a relativistic quantum field theory in the Lagrangian formulation, involving scalar, vector, and fermion fields, and indicate how to calculate amplitudes for physical processes in perturbation theory with the help of Feynman graphs. The principle of local gauge invariance is explained in terms of the well-known example of Quantum Electrodynamics (QED) with an Abelian gauge symmetry and is then generalized to the case of non-Abelian gauge invariance and applied to the formulation of Quantum Chromodynamics (QCD). In the formulation of the electroweak theory the gauge principle has to be supplemented by the concept of spontaneous symmetry breaking with the help of the Higgs field and by Yukawa interactions, for embedding massive particles in a gauge-invariant way. Excellent textbooks [5] are available for further reading.

The presentation of the structure of the electroweak Standard Model is followed by a discussion of the phenomenology of  $W$  and  $Z$  bosons and of tests of the electroweak theory at present and future colliders. The accurate predictions for the vector boson masses, cross sections, and the  $Z$  resonance observables like the width of the  $Z$  resonance, partial widths, effective neutral current coupling constants and mixing angles at the  $Z$  peak, can be compared with precise experimental data, with relevant implications for the empirically still unexplored Higgs sector. The present situation of the Higgs sector and expectations for the upcoming experiments are summarized in the final section, together with an outlook on supersymmetric Higgs bosons.

## 2 Elements of quantum field theory

### 2.1 Notations and conventions

Natural units (formally  $\hbar = c = 1$ ) are used everywhere. Lorentz indices are always denoted by greek characters,  $\mu, \nu, \dots = 0, 1, 2, 3$ . Four-vectors for space–time coordinates and particle momenta have the following contravariant components,

$$\begin{aligned}x &= (x^\mu) = (x^0, \vec{x}), & x^0 &= t, \\p &= (p^\mu) = (p^0, \vec{p}), & p^0 &= E = \sqrt{\vec{p}^2 + m^2}.\end{aligned}$$

Covariant 4-vector components are related to the contravariant components according to

$$a_\mu = g_{\mu\nu} a^\nu,$$

with the metric tensor

$$(g_{\mu\nu}) = \begin{pmatrix} 1 & 0 & 0 & 0 \\ 0 & -1 & 0 & 0 \\ 0 & 0 & -1 & 0 \\ 0 & 0 & 0 & -1 \end{pmatrix}$$

yielding the 4-dimensional squares resp. scalar products,

$$a^2 = g_{\mu\nu} a^\mu a^\nu = a_\mu a^\mu, \quad a \cdot b = a_\mu b^\mu = a^0 b^0 - \vec{a} \cdot \vec{b}.$$

Covariant and contravariant components of the derivatives are used in the following notation,

$$\begin{aligned}\partial_\mu &= \frac{\partial}{\partial x^\mu} = g_{\mu\nu} \partial^\nu, & \partial^\nu &= \frac{\partial}{\partial x_\nu} & [ \partial^0 = \partial_0, \partial^k = -\partial_k ], \\ \square &= \partial_\mu \partial^\mu = \frac{\partial^2}{\partial t^2} - \Delta.\end{aligned}$$

The quantum mechanical states of spin- $s$  particles with momentum  $p = (p^0, \vec{p})$  and helicity  $\sigma = -s, -s + 1, \dots, +s$  are denoted in the conventional way by Dirac kets  $|p \sigma\rangle$ . They are normalized according to the relativistically invariant convention

$$\langle p \sigma | p' \sigma' \rangle = 2p^0 \delta^3(\vec{p} - \vec{p}') \delta_{\sigma\sigma'}. \quad (1)$$

A special state, the zero-particle state or the vacuum, respectively, is denoted by  $|0\rangle$ . It is normalized to unity,

$$\langle 0 | 0 \rangle = 1. \quad (2)$$

### 2.2 Lagrangian formalism

The Lagrangian formalism of quantum field theory allows us to accommodate the following basic features:

- space–time symmetry in terms of Lorentz invariance, as well as internal symmetries like gauge symmetries,
- causality,
- local interactions.

Particles are described by fields that are operators on the quantum mechanical Hilbert space of the particle states, acting as creation and annihilation operators for particles and antiparticles. In the Standard Model, the following classes of particles appear, each of them described by a specific type of fields:

- spin-0 particles, described by scalar fields  $\phi(x)$ ,
- spin-1 particles, described by vector fields  $A_\mu(x)$ ,
- spin-1/2 fermions, described by spinor fields  $\psi(x)$ .

The dynamics of the physical system involving a set of fields, denoted here by a generic field variable  $\phi$ , is determined by the Lorentz-invariant Lagrangian  $\mathcal{L}$ , which yields the action

$$S[\phi] = \int d^4x \mathcal{L}(\phi(x)), \quad (3)$$

from which the equations of motions follow as Euler–Lagrange equations from Hamilton’s principle,

$$\delta S = S[\phi + \delta\phi] - S[\phi] = 0. \quad (4)$$

In particle mechanics with  $n$  generalized coordinates  $q_i$  and velocities  $\dot{q}_i$ , the Lagrangian  $L(q_1, \dots, \dot{q}_1, \dots)$  yields the equations of motion ( $i = 1, \dots, n$ )

$$\frac{d}{dt} \frac{\partial L}{\partial \dot{q}_i} - \frac{\partial L}{\partial q_i} = 0. \quad (5)$$

Proceeding to field theory, one has to perform the replacement

$$q_i \rightarrow \phi(x), \quad \dot{q}_i \rightarrow \partial_\mu \phi(x), \quad L(q_1, \dots, q_n, \dot{q}_1, \dots, \dot{q}_n) \rightarrow \mathcal{L}(\phi(x), \partial_\mu \phi(x)) \quad (6)$$

and obtains the equations of motion as field equations,

$$\partial_\mu \frac{\partial \mathcal{L}}{\partial (\partial_\mu \phi)} - \frac{\partial \mathcal{L}}{\partial \phi} = 0, \quad (7)$$

for each field (or field component), which is indicated here by the generic variable  $\phi$ .

## 2.3 Free quantum fields

### 2.3.1 Scalar fields

The Lagrangian for a free real scalar field, describing neutral spinless particles with mass  $m$ ,

$$\mathcal{L} = \frac{1}{2} (\partial_\mu \phi)^2 - \frac{m^2}{2} \phi^2 \quad (8)$$

yields the field equation according to (7), known as the *Klein–Gordon equation*,

$$(\square + m^2) \phi = 0. \quad (9)$$

The solution can be expanded in terms of the complete set of plane waves  $e^{\pm ikx}$ ,

$$\phi(x) = \frac{1}{(2\pi)^{3/2}} \int \frac{d^3k}{2k^0} [a(k) e^{-ikx} + a^\dagger(k) e^{ikx}] \quad (10)$$

with  $k^0 = \sqrt{\vec{k}^2 + m^2}$ . Constituting a quantum field, the coefficients  $a$  and the Hermitian adjoint  $a^\dagger$  are operators that annihilate and create one-particle states (see Appendix A),

$$\begin{aligned} a^\dagger(k) |0\rangle &= |k\rangle \\ a(k) |k'\rangle &= 2k^0 \delta^3(\vec{k} - \vec{k}') |0\rangle. \end{aligned} \quad (11)$$

The wave functions of one-particle states are given by the amplitudes of the field operator between the one-particle states and the vacuum,

$$\langle 0|\phi(x)|k \rangle = \frac{1}{(2\pi)^{3/2}} e^{-ikx}, \quad \langle k|\phi(x)|0 \rangle = \frac{1}{(2\pi)^{3/2}} e^{ikx}, \quad (12)$$

distinguishing between states of incoming (first) and outgoing (second) particles.

A complex scalar field  $\phi^\dagger \neq \phi$  has two degrees of freedom. It describes spinless particles which carry a charge  $\pm 1$  and can be interpreted as particles and antiparticles. The Lagrangian

$$\mathcal{L} = (\partial_\mu \phi)^\dagger (\partial^\mu \phi) - m^2 \phi^\dagger \phi \quad (13)$$

yields the field equation (9) as above, but in the Fourier expansion one has to distinguish between the annihilation and creation operators  $a, a^\dagger$  for particle states  $|+, k \rangle$  and  $b, b^\dagger$  for antiparticle states  $|-, k \rangle$ ,

$$\phi(x) = \frac{1}{(2\pi)^{3/2}} \int \frac{d^3k}{2k^0} [a(k) e^{-ikx} + b^\dagger(k) e^{ikx}] \quad (14)$$

where

$$\begin{aligned} a^\dagger(k) |0 \rangle &= |+, k \rangle, & b^\dagger(k) |0 \rangle &= |-, k \rangle \\ a(k) |+, k' \rangle &= 2k^0 \delta^3(\vec{k} - \vec{k}') |0 \rangle, & b(k) |-, k' \rangle &= 2k^0 \delta^3(\vec{k} - \vec{k}') |0 \rangle. \end{aligned} \quad (15)$$

Whereas wave functions describe free particles without space–time limitations, the important concept of the *propagator* or *Green function* is required whenever the propagation from a point-like source at a given space–time point is considered. Such a Green function  $D(x - y)$  is a solution of the inhomogeneous field equation

$$(\square + m^2) D(x - y) = -\delta^4(x - y). \quad (16)$$

The solution can easily be determined by a Fourier transformation

$$D(x - y) = \int \frac{d^4k}{(2\pi)^4} D(k) e^{-ik(x-y)} \quad (17)$$

yielding Eq. (16) in momentum space,

$$(k^2 - m^2) D(k) = 1. \quad (18)$$

The solution

$$i D(k) = \frac{i}{k^2 - m^2 + i\epsilon} \quad (19)$$

is the *causal Green function* or the *Feynman propagator* of the scalar field. The overall factor  $i$  is by convention; the term  $+i\epsilon$  in the denominator with an infinitesimal  $\epsilon > 0$  is a prescription of how to treat the pole in the integral (17); it corresponds to the special boundary condition of causality for  $D(x - y)$  in Minkowski space, which means (see Appendix B)

- propagation of a particle from  $y$  to  $x$  if  $x^0 > y^0$ ,
- propagation of an antiparticle from  $x$  to  $y$  if  $y^0 > x^0$ .

In a Feynman diagram, the propagator occurs as an internal line, whereas wave functions (resp. their Fourier transformed in momentum space) are always associated with external lines representing the physical particles in a given process. We introduce the following graphical symbol for the scalar propagator; the momentum  $k$  always points into the direction of the arrow which denotes the flow of the charge of the *particle* (for neutral fields the arrow is irrelevant).

$$i D(k) \quad \bullet \text{---} \rightarrow \text{---} \bullet \\ \qquad \qquad \qquad k$$

### 2.3.2 Vector fields

A vector field  $A_\mu(x)$  describes particles with spin 1. Their states  $|k\lambda\rangle$  can be classified by momentum  $k$  and helicity  $\lambda = \pm 1, 0$  for massive particles, and  $\lambda = \pm 1$  for particles with mass zero.

**Massive case.** For a given particle mass  $m$ , the Lagrangian for the free system ('massive photon'),

$$\mathcal{L} = -\frac{1}{4} F_{\mu\nu} F^{\mu\nu} - \frac{m^2}{2} A_\mu A^\mu \quad \text{with} \quad F_{\mu\nu} = \partial_\mu A_\nu - \partial_\nu A_\mu, \quad (20)$$

yields from (7) (with  $\phi \rightarrow A_\nu$ ) the field equation, known as the *Proca equation*,

$$[(\square + m^2) g^{\mu\nu} - \partial^\mu \partial^\nu] A_\nu = 0. \quad (21)$$

Special solutions are plane waves

$$\epsilon_\mu^{(\lambda)} e^{\pm i k x} \quad (22)$$

with three linearly independent polarization vectors  $\epsilon_\mu^{(\lambda)}$ , which are transverse and can be chosen as orthogonal and normalized,

$$\epsilon^{(\lambda)} \cdot k = 0, \quad \epsilon^{(\lambda)*} \cdot \epsilon^{(\lambda')} = -\delta_{\lambda\lambda'}, \quad (23)$$

and which fulfil the polarization sum

$$\sum_{\lambda=1}^3 \epsilon_\mu^{(\lambda)*} \epsilon_\nu^{(\lambda)} = -g_{\mu\nu} + \frac{k_\mu k_\nu}{m^2}. \quad (24)$$

The solutions (22) form a complete set, and the field  $A_\mu$  can be written as a Fourier expansion,

$$A_\mu(x) = \frac{1}{(2\pi)^{3/2}} \sum_\lambda \int \frac{d^3 k}{2k^0} [a_\lambda(k) \epsilon_\mu^{(\lambda)}(k) e^{-i k x} + a_\lambda^\dagger(k) \epsilon_\mu^{(\lambda)}(k)^* e^{i k x}]. \quad (25)$$

The coefficients are the annihilation and creation operators of particle states,

$$\begin{aligned} a_\lambda^\dagger(k) |0\rangle &= |k\lambda\rangle \\ a_\lambda(k) |k'\lambda'\rangle &= 2k^0 \delta^3(\vec{k} - \vec{k}') \delta_{\lambda\lambda'} |0\rangle. \end{aligned} \quad (26)$$

As in the scalar case, the wave functions of one-particle states are given by the amplitudes of the field operator between the one-particle states and the vacuum,

$$\langle 0 | A_\mu(x) | k\lambda \rangle = \frac{1}{(2\pi)^{3/2}} \epsilon_\mu^{(\lambda)}(k) e^{-i k x}, \quad \langle k\lambda | A_\mu(x) | 0 \rangle = \frac{1}{(2\pi)^{3/2}} \epsilon_\mu^{(\lambda)}(k)^* e^{i k x}, \quad (27)$$

corresponding to incoming and outgoing states. In momentum space, the wave functions are just the polarization vectors.

The *Feynman propagator* of the vector field,  $D_{\mu\nu}(x-y)$ , is the solution of the inhomogeneous field equation with point-like source,

$$[(\square + m^2) g^{\mu\rho} - \partial^\mu \partial^\rho] D_{\rho\nu}(x-y) = g^\mu{}_\nu \delta^4(x-y). \quad (28)$$

By Fourier transformation,

$$D_{\rho\nu}(x-y) = \int \frac{d^4 k}{(2\pi)^4} D_{\rho\nu}(k) e^{-i k(x-y)}, \quad (29)$$

one obtains an algebraic equation for  $D_{\rho\nu}(k)$ ,

$$[(-k^2 + m^2)g^{\mu\rho} + k^\mu k^\rho] D_{\rho\nu}(k) = g^\mu{}_\nu. \quad (30)$$

The solution is the Feynman propagator of a massive vector field,

$$i D_{\rho\nu}(k) = \frac{i}{k^2 - m^2 + i\epsilon} \left( -g_{\nu\rho} + \frac{k_\nu k_\rho}{m^2} \right). \quad (31)$$

As for the scalar propagator in (19), the factor  $i$  is by convention, and the  $+i\epsilon$  term in the denominator corresponds to the causal boundary condition.

**Massless case.** For particles with  $m = 0$ , like photons, the field  $A_\mu$  corresponds to the 4-potential and the Lagrangian is that of the free electromagnetic field,

$$\mathcal{L} = -\frac{1}{4} F_{\mu\nu} F^{\mu\nu} \quad \text{with} \quad F_{\mu\nu} = \partial_\mu A_\nu - \partial_\nu A_\mu. \quad (32)$$

The field equations are Maxwell's equations for the vector potential,

$$(\square g^{\mu\nu} - \partial^\mu \partial^\nu) A_\nu = 0. \quad (33)$$

There are two physical polarization vectors  $\epsilon_\mu^{(1,2)}$  for the transverse polarization, with  $\vec{\epsilon}^{(1,2)} \cdot \vec{k} = 0$ . The third solution of (33) with a longitudinal polarization vector  $\epsilon_\mu \sim k_\mu$  is unphysical; it can be removed by a gauge transformation

$$A'_\mu(x) = A_\mu(x) + \partial_\mu \chi(x) \equiv 0 \quad \text{with} \quad \chi(x) = \pm i e^{\pm i k x}. \quad (34)$$

The equation for the propagator of the massless vector field follows from (30) setting  $m = 0$ :

$$(-k^2 g^{\mu\rho} + k^\mu k^\rho) D_{\rho\nu}(k) \equiv K^{\mu\rho} D_{\rho\nu}(k) = g^\mu{}_\nu. \quad (35)$$

This equation, however, has no solution since  $K^{\mu\rho} k_\rho = 0$ , i.e.,  $k_\rho$  is an eigenvector of  $K^{\mu\rho}$  with eigenvalue 0, which means that the determinant of  $K^{\mu\rho}$  vanishes. It is therefore not straightforward to define a propagator for a massless vector field. Since the basic reason is gauge invariance, the common strategy to overcome this problem is to break the gauge symmetry by adding to  $\mathcal{L}$  a gauge-fixing term (which in classical Maxwell theory corresponds to choosing a specific gauge). Such a term, widely used for practical calculations and corresponding to the classical Lorentz gauge, has the following form,

$$\mathcal{L}_{\text{fix}} = -\frac{1}{2\xi} (\partial_\mu A^\mu)^2, \quad (36)$$

where  $\xi$  is an arbitrary real parameter, called a gauge-fixing parameter (the choice  $\xi = 1$  defines the *Feynman gauge*). The accordingly extended Lagrangian

$$\mathcal{L} = -\frac{1}{4} F_{\mu\nu} F^{\mu\nu} - \frac{1}{2\xi} (\partial_\mu A^\mu)^2 \quad (37)$$

modifies the operator  $K^{\mu\rho}$  in momentum space as follows,

$$K^{\mu\rho} \rightarrow K^{\mu\rho} - \frac{1}{\xi} k^\mu k^\rho, \quad (38)$$

and (35) is replaced by the equation,

$$\left[ -k^2 g^{\mu\rho} + \left(1 - \frac{1}{\xi}\right) k^\mu k^\rho \right] D_{\rho\nu}(k) = g^\mu{}_\nu, \quad (39)$$

which now has a solution for the massless propagator, namely

$$i D_{\rho\nu}(k) = \frac{i}{k^2 + i\epsilon} \left[ -g_{\nu\rho} + (1 - \xi) \frac{k_\nu k_\rho}{k^2} \right]. \quad (40)$$

It becomes particularly simple in the Feynman gauge for  $\xi = 1$ . Note that adding  $\mathcal{L}_{\text{fix}}$  to the Lagrangian does not have a physical impact since the induced extra terms in the propagator are  $\sim k_\nu$  and vanish in amplitudes for physical processes: photons always couple to the electromagnetic current  $j^\nu$ , which is a conserved current with  $\partial_\nu j^\nu = 0$ , or equivalently  $k_\nu j^\nu = 0$  in momentum space.

The graphical symbol for the vector-field propagator (for both massive and massless) is a wavy line which carries the momentum  $k$  and two Lorentz indices:

$$i D_{\rho\nu}(k) \quad \begin{array}{c} \bullet \text{---} \text{wavy line} \text{---} \bullet \\ \rho \qquad k \qquad \nu \end{array}$$

### 2.3.3 Dirac fields

Spin- $\frac{1}{2}$  particles, like electrons and positrons, with mass  $m$  are described by 4-component spinor fields,

$$\psi(x) = \begin{pmatrix} \psi_1(x) \\ \psi_2(x) \\ \psi_3(x) \\ \psi_4(x) \end{pmatrix}. \quad (41)$$

The dynamics of the free field is contained in the Dirac Lagrangian,

$$\mathcal{L} = \bar{\psi} (i\gamma^\mu \partial_\mu - m) \psi, \quad (42)$$

involving the adjoint spinor

$$\bar{\psi} = \psi^\dagger \gamma^0 = (\psi_1^*, \psi_2^*, -\psi_3^*, -\psi_4^*). \quad (43)$$

The Dirac matrices  $\gamma^\mu$  ( $\mu = 0, 1, 2, 3$ ) are  $4 \times 4$  matrices which can be written with the help of the Pauli matrices  $\sigma_{1,2,3}$  in the following way (the Dirac representation),

$$\gamma^0 = \begin{pmatrix} \mathbf{1} & 0 \\ 0 & -\mathbf{1} \end{pmatrix}, \quad \gamma^k = \begin{pmatrix} 0 & \sigma_k \\ -\sigma_k & 0 \end{pmatrix}. \quad (44)$$

They fulfil the anti-commutator relations

$$\{\gamma^\mu, \gamma^\nu\} \equiv \gamma^\mu \gamma^\nu + \gamma^\nu \gamma^\mu = 2g^{\mu\nu}. \quad (45)$$

The Lagrangian (42) yields the *Dirac equation* as the equation of motion,

$$(i\gamma^\mu \partial_\mu - m) \psi = 0. \quad (46)$$

There are two types of solutions, corresponding to particle and anti-particle wave functions,

$$u(p) e^{-ipx} \quad \text{and} \quad v(p) e^{ipx} \quad (47)$$

where the spinors  $u$  and  $v$  fulfil the algebraic equations

$$(\not{p} - m)u(p) = 0, \quad (\not{p} + m)v(p) = 0. \quad (48)$$

Thereby, the notation  $\not{a} = \gamma^\mu a_\mu$  applying to any 4-vector  $a_\mu$  has been used. The solutions (48) correspond to momentum eigenstates with eigenvalue  $p^\mu$ . They can further be classified as helicity states with helicity  $\sigma = \pm 1/2$  by the requirement

$$\frac{1}{2} (\vec{\Sigma} \cdot \vec{n}) u_\sigma(p) = \sigma u_\sigma(p), \quad -\frac{1}{2} (\vec{\Sigma} \cdot \vec{n}) v_\sigma(p) = \sigma v_\sigma(p) \quad (49)$$

with

$$\vec{\Sigma} = \begin{pmatrix} \vec{\sigma} & 0 \\ 0 & \vec{\sigma} \end{pmatrix} \quad \text{and} \quad \vec{n} = \frac{\vec{p}}{|\vec{p}|}. \quad (50)$$

The normalization of the spinors is given by

$$\bar{u}_\sigma u_{\sigma'} = 2m \delta_{\sigma\sigma'}, \quad \bar{v}_\sigma v_{\sigma'} = -2m \delta_{\sigma\sigma'}. \quad (51)$$

Other useful relations are

$$\sum_\sigma u_\sigma \bar{u}_\sigma = \not{p} + m, \quad \sum_\sigma v_\sigma \bar{v}_\sigma = \not{p} - m. \quad (52)$$

Having determined a complete set of solutions of the Dirac equation (46), we can now write the Dirac quantum field as an expansion in terms of these solutions,

$$\psi(x) = \frac{1}{(2\pi)^{3/2}} \sum_\sigma \int \frac{d^3k}{2k^0} [c_\sigma(k) u_\sigma(k) e^{-ikx} + d_\sigma^\dagger(k) v_\sigma(k) e^{ikx}], \quad (53)$$

where the coefficients are annihilation operators  $c_\sigma$  for particles and  $d_\sigma$  for anti-particles, as well as creation operators  $c_\sigma^\dagger$  and  $d_\sigma^\dagger$  for particles and antiparticles, respectively. In QED, electrons  $e^-$  are by convention the particles and positrons the antiparticles. Choosing the  $e^\pm$  field as a concrete example, we thus have

$$\begin{aligned} c_\sigma^\dagger(k) |0\rangle &= |e^-, k\sigma\rangle, & d_\sigma^\dagger(k) |0\rangle &= |e^+, k\sigma\rangle \\ c_\sigma(k) |e^-, k'\sigma'\rangle &= 2k^0 \delta^3(\vec{k} - \vec{k}') \delta_{\sigma\sigma'} |0\rangle, & d_\sigma(k) |e^+, k'\sigma'\rangle &= 2k^0 \delta^3(\vec{k} - \vec{k}') \delta_{\sigma\sigma'} |0\rangle. \end{aligned} \quad (54)$$

There are four types of wave functions, for incoming and outgoing particles and antiparticles,

$$\begin{aligned} \langle 0|\psi(x)|e^-, k\sigma\rangle &= \frac{1}{(2\pi)^{3/2}} u_\sigma(k) e^{-ikx}, & \langle e^+, k\sigma|\psi(x)|0\rangle &= \frac{1}{(2\pi)^{3/2}} v_\sigma(k) e^{ikx}, \\ \langle 0|\bar{\psi}(x)|e^+, k\sigma\rangle &= \frac{1}{(2\pi)^{3/2}} \bar{v}_\sigma(k) e^{-ikx}, & \langle e^-, k\sigma|\bar{\psi}(x)|0\rangle &= \frac{1}{(2\pi)^{3/2}} \bar{u}_\sigma(k) e^{ikx}. \end{aligned} \quad (55)$$

In momentum space, dropping the  $(2\pi)^{-3/2}$  factors and the helicity indices, we describe the situations as follows using a graphical notation ( $k$  always denotes the physical momentum flowing towards an interaction point for incoming and off an interaction point for outgoing states),

|                       |              |                   |                   |
|-----------------------|--------------|-------------------|-------------------|
| incoming particle     | $u(k)$       | $\longrightarrow$ | $\bullet$         |
| incoming antiparticle | $\bar{v}(k)$ | $\longleftarrow$  | $\bullet$         |
| outgoing antiparticle | $v(k)$       | $\bullet$         | $\longleftarrow$  |
| outgoing particle     | $\bar{u}(k)$ | $\bullet$         | $\longrightarrow$ |

The arrows indicate the flow of the *particle* charge. Note that for antiparticles the direction of the momentum is opposite to the arrow at the line.

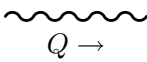
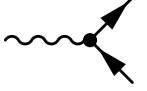
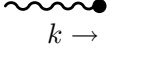
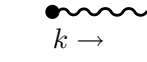
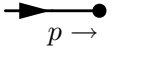
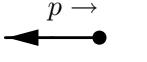
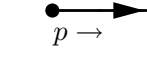
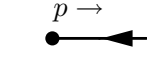
We still have to determine the propagator of the Dirac field, which is the solution of the inhomogeneous Dirac equation with point-like source,

$$(i\gamma^\mu \partial_\mu - m) S(x - y) = \mathbf{1} \delta^4(x - y). \quad (56)$$



Note that the factor  $i$  is a convention. The lines can be either propagators (internal) or wave functions (external) in momentum space. They carry momenta which have to fulfil momentum conservation. Formally, momentum conservation follows via Fourier transformation from the exponentials in the wave functions (27,55) and the propagators (29,57) when going to momentum space.

Collecting all the information, we give the complete list of Feynman rules for QED, with the photon propagator in the Feynman gauge. For fermions different from  $e$  (or  $\mu, \tau$ ), an extra factor for the different charge appears in the vertex, as indicated in the brackets. Helicity indices are suppressed for the wave functions.

|   |                                      |                                 |
|---|--------------------------------------|---------------------------------|
|    | $\frac{-ig_{\mu\nu}}{Q^2+i\epsilon}$ | photon propagator ( $\xi = 1$ ) |
|    | $i\frac{Q+m}{Q^2-m^2+i\epsilon}$     | fermion propagator              |
|    | $ie\gamma^\mu(Q_f)$                  | electron–photon vertex          |
|    | $\epsilon_\mu(k)$                    | incoming photon                 |
|    | $\epsilon_\mu^*(k)$                  | outgoing photon                 |
|  | $u(p)$                               | incoming fermion                |
|  | $\bar{v}(p)$                         | incoming anti-fermion           |
|  | $\bar{u}(p)$                         | outgoing fermion                |
|  | $v(p)$                               | outgoing anti-fermion           |

To obtain the transition matrix element, the amplitude  $\mathcal{M}_{fi}$  for a physical process  $|i\rangle \rightarrow |f\rangle$  (see Section 3), one has the following recipe.

- For a process with given external particles draw all diagrams connecting the external lines by vertices and propagators. The lowest order corresponds to diagrams involving the minimum number of vertices, which determines the power of the coupling constant  $e$  in the matrix element.
- Insert the analytical expressions for the wave functions, propagators and vertices from the Feynman rules. The arrangement of spinors is thereby opposite to the arrow at a fermion line.
- Impose momentum conservation at each vertex.
- Sum over all diagrams, paying attention to the relative sign which occurs when two fermion lines are interchanged (according to Pauli's principle).

Note that the factors  $(2\pi)^{-3/2}$  from each wave function are omitted so far. They are collected globally and reappear in the  $S$ -matrix element and the cross section, respectively (Section 3.1) We demonstrate the method for the process of electron–positron annihilation into muon pairs,  $e^+e^- \rightarrow \mu^+\mu^-$ . There is only one Feynman diagram in lowest order, displayed in Fig. 1. The analytical expression for the amplitude according to this diagram is given by

$$\mathcal{M}_{fi} = \bar{v}(q)ie\gamma^\mu u(p) \left( \frac{-ig_{\mu\nu}}{Q^2+i\epsilon} \right) \bar{u}(p')ie\gamma^\nu v(q') = i\frac{e^2}{Q^2} \bar{v}(q)\gamma^\mu u(p) \bar{u}(p')\gamma^\nu v(q'). \quad (63)$$

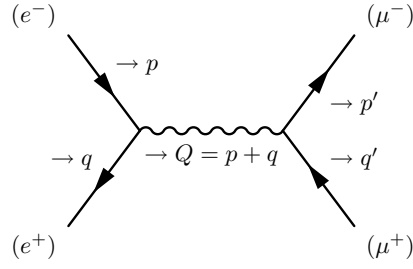


**Fig. 1:** Lowest-order Feynman graph for  $e^+e^- \rightarrow \mu^+\mu^-$ . The momenta with directions are indicated at each line.

Since  $Q^2 = (p + q)^2 > 4m_\mu^2$ , the  $i\epsilon$  term in the photon propagator is irrelevant and can be dropped.

The next-order contribution to  $\mathcal{M}_{fi}$ , which is  $\sim e^4$ , contains diagrams with closed loops. Examples are displayed in Fig. 2. Since inside a loop one momentum is free, not fixed by momentum conservation, loop diagrams involve a 4-dimensional integration over the free momentum (Section 7.2.1).

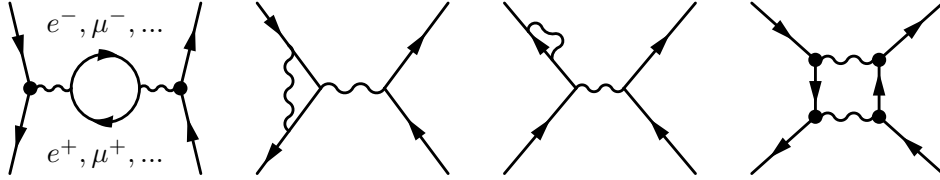


**Fig. 2:** One-loop order Feynman graphs for  $e^+e^- \rightarrow \mu^+\mu^-$  (examples)

### 3 Cross sections and decay rates

This section provides the kinematical relations necessary for getting from the matrix elements for physical processes to observable quantities, like cross sections and decay rates.

#### 3.1 Scattering processes

For a given scattering process  $a + b \rightarrow b_1 + b_2 + \dots + b_n$  the  $S$ -matrix element  $S_{fi} = \langle f|S|i \rangle$  is the probability amplitude for the transition from an initial state  $|a(p_a), b(p_b)\rangle = |i\rangle$  to a final state  $|b_1(p_1), \dots, b_n(p_n)\rangle = |f\rangle$  of free particles. For  $|i\rangle \neq |f\rangle$ , one can write

$$S_{fi} = (2\pi)^4 \delta^4(P_i - P_f) \mathcal{M}_{fi} (2\pi)^{-3(n+2)/2} \quad (64)$$

with the  $\delta$ -function from momentum conservation,

$$P_i = p_a + p_b = P_f = p_1 + \dots + p_n, \quad (65)$$

the  $(2\pi)^{-3/2}$  factors from the normalization of the external wave functions, and with the genuine matrix element  $\mathcal{M}_{fi}$  derived from the Feynman graphs for the scattering process. The differential cross section for scattering into the Lorentz-invariant phase space element

$$d\Phi = \frac{d^3p_1}{2p_1^0} \dots \frac{d^3p_n}{2p_n^0} \quad (66)$$

is given by

$$d\sigma = \frac{(2\pi)^4}{4\sqrt{(p_a \cdot p_b)^2 - m_a^2 m_b^2}} |\mathcal{M}_{fi}|^2 (2\pi)^{-3n} \delta^4(P_i - P_f) d\Phi. \quad (67)$$

The expression in the denominator is the relativistically-invariant version of the incoming flux-normalization factor. As a special example of practical importance, we give the cross section for a two-particle final state  $a + b \rightarrow b_1 + b_2$  in the centre-of-mass system (CMS), where  $\vec{p}_a + \vec{p}_b = 0 = \vec{p}_1 + \vec{p}_2$ :

$$\frac{d\sigma}{d\Omega} = \frac{1}{64\pi^2 s} \frac{|\vec{p}_1|}{|\vec{p}_a|} |\mathcal{M}_{fi}|^2 \quad (68)$$

with  $s = (p_a + p_b)^2 = (p_a^0 + p_b^0)^2$  and the solid angle  $d\Omega = \sin\theta d\theta d\varphi$  involving the scattering angle  $\theta = \langle \vec{p}_a, \vec{p}_1 \rangle$ , and the azimuth  $\varphi$  with respect to the polar axis given by  $\vec{p}_a$ . For high energies, when the particle masses are negligible, one has the further simplification  $|\vec{p}_1| = |\vec{p}_a|$ .

### 3.2 Particle decays

For a decay process  $a \rightarrow b_1 + b_2 + \dots + b_n$  where  $|a(p_a)\rangle = |i\rangle$ ,  $|b_1(p_1), \dots, b_n(p_n)\rangle = |f\rangle$ , the (differential) decay width into the phase space element  $d\Phi$  is given by

$$d\Gamma = \frac{(2\pi)^4}{2m_a} |\mathcal{M}_{fi}|^2 (2\pi)^{-3n} \delta^4(p_a - P_f) d\Phi. \quad (69)$$

In the special case of a two-particle decay with final-state masses  $m_1 = m_2 = m$  one has the simple expression

$$\frac{d\Gamma}{d\Omega} = \frac{1}{64\pi^2 m_a} \sqrt{1 - \frac{4m^2}{m_a^2}} |\mathcal{M}_{fi}|^2. \quad (70)$$

## 4 Gauge theories

The powerful principle of gauge invariance dictates the structure of the interactions between fermions and vector bosons as well as the vector boson self-interactions. It is the generalization of the Abelian gauge symmetry found in Quantum Electrodynamics (QED) to the non-Abelian case.

### 4.1 Abelian gauge theories — QED

QED can be derived by the requirement that the global  $U(1)$  symmetry of the Lagrangian for the free charged fermion field  $\psi$ , i.e., the symmetry of

$$\mathcal{L}_0 = \bar{\psi} (\gamma^\mu \partial_\mu - m) \psi \quad (71)$$

under the phase transformation

$$\psi(x) \rightarrow \psi'(x) = e^{i\alpha} \psi(x) \quad (72)$$

for arbitrary real numbers  $\alpha$ , can be extended to a symmetry under local transformations where  $\alpha \rightarrow \alpha(x)$  is now an arbitrary real function. This necessitates the presence of a vector field  $A_\mu$  and the *minimal substitution* of the derivative in  $\mathcal{L}_0$  by the *covariant derivative*

$$\partial_\mu \rightarrow D_\mu = \partial_\mu - ieA_\mu, \quad (73)$$

yielding a Lagrangian that is invariant under the local gauge transformations

$$\psi(x) \rightarrow \psi'(x) = e^{i\alpha(x)} \psi(x),$$

$$A_\mu(x) \rightarrow A'_\mu(x) = A_\mu(x) + \frac{1}{e} \partial_\mu \alpha(x), \quad (74)$$

which form the electromagnetic gauge group  $U(1)$ . As an immediate consequence, the invariant Lagrangian describes an interaction of the vector field with the electromagnetic current (62),

$$\mathcal{L} = \bar{\psi} (i\gamma^\mu D_\mu - m) \psi = \mathcal{L}_0 + e \bar{\psi} \gamma^\mu \psi A_\mu = \mathcal{L}_0 + \mathcal{L}_{int}. \quad (75)$$

The vector field  $A_\mu$  itself is not yet a dynamical field since a kinetic term is still missing. Such a term can easily be added invoking the expression well known from classical electrodynamics,

$$\mathcal{L}_A = -\frac{1}{4} F_{\mu\nu} F^{\mu\nu} \quad \text{with the field strengths} \quad F_{\mu\nu} = \partial_\mu A_\nu - \partial_\nu A_\mu, \quad (76)$$

which is invariant under the local gauge transformation (74).  $A_\mu$  thus becomes the photon field obeying Maxwell's equations.

## 4.2 Non-Abelian gauge theories

The three basic steps yielding QED as the gauge theory of the electromagnetic interaction:

- (i) identifying the global symmetry of the free Lagrangian,
- (ii) replacing  $\partial_\mu$  via minimal substitution by the covariant derivative  $D_\mu$  with a vector field,
- (iii) adding a kinetic term for the vector field,

can now be extended to the case of non-Abelian symmetries as follows.

(i) The given non-interacting system is described by a multiplet of fermion fields with mass  $m$ ,  $\Psi = (\psi_1, \psi_2, \dots, \psi_n)^T$ , and the free dynamics by the Lagrangian

$$\mathcal{L}_0 = \bar{\Psi} (\gamma^\mu \partial_\mu - m) \Psi \quad \text{with} \quad \bar{\Psi} = (\bar{\psi}_1, \dots, \bar{\psi}_n). \quad (77)$$

$\mathcal{L}_0$  is invariant under global transformations

$$\Psi(x) \rightarrow U(\alpha^1, \dots, \alpha^N) \Psi(x), \quad (78)$$

with unitary matrices  $U$  from an  $n$ -dimensional representation of a non-Abelian Lie group  $G$  of rank  $N$ , depending on  $N$  real parameters  $\alpha^1, \dots, \alpha^N$ . Physically relevant cases are  $G = SU(2)$  and  $G = SU(3)$ , where the fermion fields  $\psi_1, \dots, \psi_n$  form the fundamental representations with  $n = 2$  and  $n = 3$ , respectively.

The matrices  $U$  can be written as follows,

$$U(\alpha^1, \dots, \alpha^N) = e^{i(\alpha^1 T_1 + \dots + \alpha^N T_N)}, \quad (79)$$

with the generators of the Lie group,  $T_1, \dots, T_N$ . These Hermitian matrices form the Lie algebra

$$[T_a, T_b] = i f_{abc} T_c \quad (80)$$

with the structure constants  $f_{abc}$  as real numbers characteristic for the group. Conventionally, the generators are normalized according to

$$\text{Tr}(T_a T_b) = \frac{1}{2} \delta_{ab}. \quad (81)$$

(ii) The global symmetry can now be extended to a local symmetry by converting the constants  $\alpha^a$  in (79) to real functions  $\alpha^a(x)$ ,  $a = 1, \dots, N$ , and simultaneously introducing a covariant derivative in (77), via

$$\partial_\mu \rightarrow D_\mu = \partial_\mu - ig \mathbf{W}_\mu, \quad (82)$$

involving a vector field  $\mathbf{W}_\mu$ , together with a coupling constant  $g$  (the analogue of  $e$  in QED). Since  $D_\mu$  acts on the  $n$ -dimensional column  $\Psi$ , the vector field is a  $n \times n$  matrix and can be expanded in terms of the generators,

$$\mathbf{W}_\mu(x) = T_a W_\mu^a(x) \quad (\text{summation over } a = 1, \dots, N). \quad (83)$$

In this way, a set of  $N$  fields  $W_\mu^a(x)$ , the gauge fields, enters the Lagrangian (77) and induces an interaction term,

$$\mathcal{L}_0 \rightarrow \mathcal{L} = \mathcal{L}_0 + \mathcal{L}_{\text{int}} \quad \text{with} \quad \mathcal{L}_{\text{int}} = g \bar{\Psi} \gamma^\mu \mathbf{W}_\mu \Psi = g \bar{\Psi} \gamma^\mu T_a \Psi W_\mu^a, \quad (84)$$

which contains the interaction of  $N$  currents  $j_a^\mu = g \bar{\Psi} \gamma^\mu T_a \Psi$  with the gauge fields  $W_\mu^a$ .

The local gauge transformation that leaves  $\mathcal{L}$  invariant, involves the matrix  $U \equiv U(\alpha^1(x), \dots)$  and reads as follows,

$$\begin{aligned} \Psi &\rightarrow \Psi' = U \Psi, \\ \mathbf{W}_\mu &\rightarrow \mathbf{W}'_\mu = U \mathbf{W}_\mu U^{-1} - \frac{i}{g} (\partial_\mu U) U^{-1}. \end{aligned} \quad (85)$$

The gauge transformation for the vector field looks more familiar when written for the components and expanded for infinitesimal  $\alpha^a(x)$ :

$$W_\mu^a \rightarrow W'^a_\mu = W_\mu^a + \frac{1}{g} \partial_\mu \alpha^a + f_{abc} W_\mu^b \alpha^c. \quad (86)$$

The derivative term corresponds to (74) in the Abelian case, the last term is of pure non-Abelian origin.

Note: The construction works in the same way for a multiplet of scalar fields  $\Phi = (\phi_1, \dots, \phi_n)^T$ , with

$$\mathcal{L}_0 = (\partial_\mu \Phi)^\dagger (\partial^\mu \Phi) - m^2 \Phi^\dagger \Phi \quad \rightarrow \quad \mathcal{L} = (D_\mu \Phi)^\dagger (D^\mu \Phi) - m^2 \Phi^\dagger \Phi. \quad (87)$$

(iii) The kinetic term for the  $W$  fields can be obtained from a generalization of the electromagnetic field strength tensor  $F_{\mu\nu}$  in (76),

$$\mathbf{F}_{\mu\nu} = T_a F_{\mu\nu}^a = \partial_\mu \mathbf{W}_\nu - \partial_\nu \mathbf{W}_\mu - i g [\mathbf{W}_\mu, \mathbf{W}_\nu], \quad (88)$$

with the  $N$  components

$$F_{\mu\nu}^a = \partial_\mu W_\nu^a - \partial_\nu W_\mu^a + g f_{abc} W_\mu^b W_\nu^c. \quad (89)$$

Under the gauge transformation (85) the field strength is transformed according to

$$\mathbf{F}_{\mu\nu} \rightarrow \mathbf{F}'_{\mu\nu} = U \mathbf{F}_{\mu\nu} U^{-1}. \quad (90)$$

As a consequence, the trace  $\text{Tr}(\mathbf{F}_{\mu\nu} \mathbf{F}^{\mu\nu})$  is gauge invariant,

$$\text{Tr}(\mathbf{F}'_{\mu\nu} \mathbf{F}'^{\mu\nu}) = \text{Tr}(U \mathbf{F}_{\mu\nu} U^{-1} U \mathbf{F}^{\mu\nu} U^{-1}) = \text{Tr}(U^{-1} U \mathbf{F}_{\mu\nu} U^{-1} U \mathbf{F}^{\mu\nu}) = \text{Tr}(\mathbf{F}_{\mu\nu} \mathbf{F}^{\mu\nu}), \quad (91)$$

and provides the non-Abelian analogue of (76) for the kinetic term of the gauge fields  $W_\mu^a$ ,

$$\mathcal{L}_W = -\frac{1}{2} \text{Tr}(\mathbf{F}_{\mu\nu} \mathbf{F}^{\mu\nu}) = -\frac{1}{4} F_{\mu\nu}^a F^{a,\mu\nu}. \quad (92)$$

The quadratic part of  $\mathcal{L}_W$  describes the free propagation of the  $W$  fields, but there are also cubic and quartic terms describing self-interactions of the vector fields that are determined exclusively through the gauge symmetry:

$$\mathcal{L}_W = -\frac{1}{4} (\partial_\mu W_\nu^a - \partial_\nu W_\mu^a) (\partial^\mu W^{a,\nu} - \partial^\nu W^{a,\mu})$$

$$\begin{aligned}
& -\frac{g}{2} f_{abc} (\partial_\mu W_\nu^a - \partial_\nu W_\mu^a) W^{b,\mu} W^{c,\nu} \\
& -\frac{g^2}{4} f_{abc} f_{ade} W_\mu^b W_\nu^c W^{d,\mu} W^{e,\nu}.
\end{aligned} \tag{93}$$

In the gauge field Lagrangians  $\mathcal{L}_W$  and  $\mathcal{L}_A$ , the vector fields are strictly massless. Mass terms  $\frac{m^2}{2} W_\mu^a W^{a,\mu}$  are not invariant under gauge transformations and thus would break the gauge symmetry.

## 5 Formulation of QCD

Quantum Chromodynamics (QCD), the gauge theory of the strong interaction, is formulated following the principle of the previous section for the specific case of the symmetry group  $G = SU(3)$ . The basic fermions are quarks in three different colour states, forming the fundamental representation of the group. They are described by triplets of fermion fields  $\Psi = (q_1, q_2, q_3)^T$  for each quark flavor  $u, d, \dots$ . The colour group  $SU(3)$  has eight generators  $T_a$ , which in the triplet representation

$$T_a = \frac{1}{2} \lambda_a, \quad a = 1, \dots, 8, \tag{94}$$

are expressed in terms of eight  $3 \times 3$  matrices, the Gell-Mann matrices  $\lambda_a$ . The covariant derivative, acting on the quark triplets  $\Psi$ ,

$$D_\mu = \partial_\mu - ig_s \frac{\lambda_a}{2} G_\mu^a, \tag{95}$$

and the field strengths

$$G_{\mu\nu}^a = \partial_\mu G_\nu^a - \partial_\nu G_\mu^a + g_s f_{abc} G_\mu^b G_\nu^c, \tag{96}$$

involve eight gauge fields, the gluon fields  $G_\mu^a$ , and the coupling constant of QCD, the strong coupling constant  $g_s$ , which is commonly expressed in terms of the finestructure constant of the strong interaction,

$$\alpha_s = \frac{g_s^2}{4\pi}. \tag{97}$$

The Lagrangian of QCD (for a given species of quarks) can then easily be written down according to the rules of Section 4 (see also Ref. [6]),

$$\begin{aligned}
\mathcal{L}_{\text{QCD}} &= \bar{\Psi} (i\gamma^\mu D_\mu - m)\Psi + \mathcal{L}_G \\
&= \bar{\Psi} (i\gamma^\mu \partial_\mu - m)\Psi + g_s \bar{\Psi} \gamma^\mu \frac{\lambda_a}{2} \Psi G_\mu^a - \frac{1}{4} G_{\mu\nu}^a G^{a,\mu\nu}.
\end{aligned} \tag{98}$$

It involves the interaction of the quark currents with the gluon fields as well as the triple and quartic gluon self interactions as specified in (93), graphically displayed as Feynman rules for QCD in Fig. 3. There is also a gauge-fixing term in the Lagrangian for each gluon field (not explicitly written here), which can be chosen in the same way as for the photon field in (36) yielding the same form for the gluon propagators as for the photon propagator in (40).

The quark mass  $m$  appears in QCD as a free parameter for a given colour triplet. It is different for different quark flavours; its origin is of electroweak nature and will be discussed in the subsequent section.

Note that the Lagrangian above considers only a single species of flavour. For the realistic physical situation of six flavours, one has to introduce a colour triplet for each flavour  $q = u, d, \dots, t$  and to perform a summation over  $q$ , with individual masses  $m_q$ .

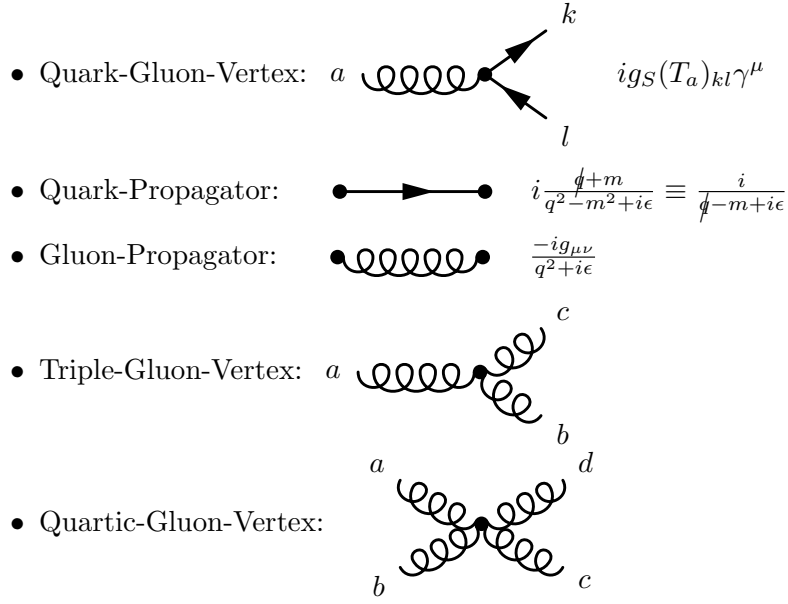


**Fig. 3:** Propagators and interactions in QCD

## 6 Formulation of the electroweak Standard Model

The fundamental fermions, as families of leptons and quarks with left-handed doublets and right-handed singlets, appear as the fundamental representations of the group  $SU(2) \times U(1)$ ,

$$\begin{aligned} & \begin{pmatrix} \nu_e \\ e \end{pmatrix}_L, \quad \begin{pmatrix} \nu_\mu \\ \mu \end{pmatrix}_L, \quad \begin{pmatrix} \nu_\tau \\ \tau \end{pmatrix}_L, \quad e_R, \quad \mu_R, \quad \tau_R \\ & \begin{pmatrix} u \\ d \end{pmatrix}_L, \quad \begin{pmatrix} c \\ s \end{pmatrix}_L, \quad \begin{pmatrix} t \\ b \end{pmatrix}_L, \quad u_R, \quad d_R, \quad c_R, \quad s_R, \quad t_R, \quad b_R \end{aligned} \quad (99)$$

They can be classified by the quantum numbers of the weak isospin  $I$ ,  $I_3$ , and the weak hypercharge  $Y$ . Left-handed fields have  $I = \frac{1}{2}$  and thus form doublets, right-handed fields are singlets with  $I = 0$ . The Gell-Mann–Nishijima relation establishes the relation of these basic quantum numbers to the electric charge  $Q$ :

$$Q = I_3 + \frac{Y}{2}. \quad (100)$$

The assignment of the quantum numbers to the fundamental lepton and quark fields is contained in Table 1 for the fermions of the first generation (identical for the second and third generation).

This structure can be embedded in a gauge invariant field theory of the unified electromagnetic and weak interactions by interpreting  $SU(2) \times U(1)$  as the group of gauge transformations under which

**Table 1:** Quantum numbers isospin  $I_3$  and hypercharge  $Y$  for the left- and right-handed leptons and quarks, together with the electric charge  $Q$

|       | $\nu_L$ | $e_L$ | $e_R$ | $u_L$ | $d_L$ | $u_R$ | $d_R$ |
|-------|---------|-------|-------|-------|-------|-------|-------|
| $I_3$ | +1/2    | -1/2  | 0     | +1/2  | -1/2  | 0     | 0     |
| $Y$   | -1      | -1    | -2    | +1/3  | +1/3  | +4/3  | -2/3  |
| $Q$   | 0       | -1    | -1    | +2/3  | -1/3  | +2/3  | -1/3  |

the Lagrangian is invariant. The group has four generators,

$$T_a = I_a \quad (a = 1, 2, 3) \quad \text{and} \quad T_4 = Y, \quad (101)$$

where  $Y$  is the Abelian hypercharge, and  $I_a$  are the isospin operators, forming the Lie algebra

$$[I_a, I_b] = i \epsilon_{abc} I_c, \quad [I_a, Y] = 0. \quad (102)$$

This electroweak symmetry has to be broken down to the electromagnetic gauge symmetry  $U(1)_{\text{em}}$ , otherwise the  $W^\pm$ ,  $Z$  bosons would be massless. In the Standard Model, this is done by the Higgs mechanism in its minimal formulation requiring a single Higgs field which is a doublet under  $SU(2)$ .

According to the general principles of constructing a gauge-invariant field theory with spontaneous symmetry breaking, the gauge, Higgs, fermion and Yukawa parts of the electroweak Lagrangian

$$\mathcal{L}_{\text{EW}} = \mathcal{L}_G + \mathcal{L}_H + \mathcal{L}_F + \mathcal{L}_Y \quad (103)$$

are specified in the following way.

**Gauge fields.**  $SU(2) \times U(1)$  is a non-Abelian group with generators  $I_a, Y$ , where  $I_a$  ( $a = 1, 2, 3$ ) are the isospin operators and  $Y$  is the hypercharge. Each of these generalized charges is associated with a vector field: a triplet of vector fields  $W_\mu^{1,2,3}$  with  $I_{1,2,3}$ , and a singlet field  $B_\mu$  with  $Y$ . The isotriplet  $W_\mu^a$  and the isosinglet  $B_\mu$  lead to the field strength tensors

$$\begin{aligned} W_{\mu\nu}^a &= \partial_\mu W_\nu^a - \partial_\nu W_\mu^a + g_2 \epsilon_{abc} W_\mu^b W_\nu^c, \\ B_{\mu\nu} &= \partial_\mu B_\nu - \partial_\nu B_\mu. \end{aligned} \quad (104)$$

Since the gauge group is semi-simple and contains two factors, there are two independent gauge coupling constants, denoted by  $g_2$  for the non-Abelian factor  $SU(2)$  and by  $g_1$  for the Abelian factor  $U(1)$ . From the field tensors (104) the pure gauge field Lagrangian

$$\mathcal{L}_G = -\frac{1}{4} W_{\mu\nu}^a W^{\mu\nu,a} - \frac{1}{4} B_{\mu\nu} B^{\mu\nu} \quad (105)$$

is constructed, which is invariant under gauge transformations composed of (85) and (74). Explicit mass terms for the gauge fields are forbidden because they violate gauge invariance. Masses for the vector bosons of the weak interaction will be introduced in a second step below by breaking the electroweak symmetry spontaneously with the help of the Higgs mechanism.

**Fermion fields and fermion–gauge interactions.** Since the representations of the gauge group are different for fermions with different chirality, we have to distinguish between the left- and right-handed fields. We use the generic notation for the chiral fields,

$$\psi_L = \frac{1 - \gamma_5}{2} \psi, \quad \psi_R = \frac{1 + \gamma_5}{2} \psi. \quad (106)$$

The left-handed fermion fields of each lepton and quark family with generation index  $j$  are grouped into  $SU(2)$  doublets and the right-handed fields into singlets,

$$\psi_L^j = \begin{pmatrix} \psi_{L+}^j \\ \psi_{L-}^j \end{pmatrix}, \quad \psi_{R\sigma}^j \quad (107)$$

with the component index  $\sigma = \pm$  denoting  $u$ -type fermions (+) and  $d$ -type fermions (–). Each left- and right-handed multiplet is an eigenstate of the weak hypercharge  $Y$  such that the relation (100) is fulfilled (see Table 1). The covariant derivative

$$D_\mu^{L,R} = \partial_\mu - i g_2 I_a^{L,R} W_\mu^a + i g_1 \frac{Y}{2} B_\mu \quad \text{with} \quad I_a^L = \frac{1}{2} \sigma_a, \quad I_a^R = 0 \quad (108)$$

induces the fermion–gauge field interaction via the minimal substitution rule,

$$\mathcal{L}_F = \sum_j \bar{\psi}_L^j i\gamma^\mu D_\mu^L \psi_L^j + \sum_{j,\sigma} \bar{\psi}_{R\sigma}^j i\gamma^\mu D_\mu^R \psi_{R\sigma}^j, \quad (109)$$

where the index  $j$  runs over the three lepton and quark generations (99). Note that the covariant derivatives are different for the  $L$  and  $R$  fields.

Mass terms are avoided at this stage. They would mix left- and right-handed fields as, for example, in  $m_e(\bar{e}_L e_R + \bar{e}_R e_L)$  and hence would explicitly break gauge invariance. They will be introduced later with the help of gauge-invariant Yukawa interactions of the fermions with the Higgs field. Note that in the genuine Standard Model neutrinos are considered as massless and there are no right-handed neutrino fields.

**Higgs field and Higgs interactions.** Here we describe how spontaneous breaking of the  $SU(2) \times U(1)$  symmetry can be obtained, leaving the electromagnetic gauge subgroup  $U(1)_{\text{em}}$  unbroken. For this aim, a single isospin doublet of complex scalar fields with hypercharge  $Y = 1$ ,

$$\Phi(x) = \begin{pmatrix} \phi^+(x) \\ \phi^0(x) \end{pmatrix}, \quad (110)$$

is introduced and coupled to the gauge fields via minimal substitution as indicated in (87),

$$\mathcal{L}_H = (D_\mu \Phi)^\dagger (D^\mu \Phi) - V(\Phi), \quad (111)$$

with the covariant derivative for  $I = \frac{1}{2}$  and  $Y = 1$  given by

$$D_\mu = \partial_\mu - i g_2 \frac{\sigma_a}{2} W_\mu^a + i \frac{g_1}{2} B_\mu. \quad (112)$$

The Higgs field self-interaction enters through the Higgs potential with constants  $\mu^2$  and  $\lambda$ ,

$$V(\Phi) = -\mu^2 \Phi^\dagger \Phi + \frac{\lambda}{4} (\Phi^\dagger \Phi)^2. \quad (113)$$

In the ground state, the vacuum, the potential has a minimum. For  $\mu^2, \lambda > 0$ , the minimum does not occur for  $\Phi = 0$ ; instead,  $V$  is minimized by all non-vanishing field configurations with  $\Phi^\dagger \Phi = 2\mu^2/\lambda$ . Selecting the one which is real and electrically neutral,  $Q\Phi = 0$ , with

$$Q = I_3 + \frac{Y}{2} = \begin{pmatrix} 1 & 0 \\ 0 & 0 \end{pmatrix}, \quad (114)$$

one gets the *vacuum expectation value*

$$\langle \Phi \rangle = \frac{1}{\sqrt{2}} \begin{pmatrix} 0 \\ v \end{pmatrix} \quad \text{with} \quad v = \frac{2\mu}{\sqrt{\lambda}}. \quad (115)$$

Although the Lagrangian is symmetric under gauge transformations of the full  $SU(2) \times U(1)$  group, the vacuum configuration  $\langle \Phi \rangle$  does not have this symmetry: the symmetry has been *spontaneously broken*.  $\langle \Phi \rangle$  is still symmetric under transformations of the electromagnetic subgroup  $U(1)_{\text{em}}$ , which is generated by the charge  $Q$ , thus preserving the electromagnetic gauge symmetry.

The field (110) can be written in the following way,

$$\Phi(x) = \begin{pmatrix} \phi^+(x) \\ (v + H(x) + i\chi(x))/\sqrt{2} \end{pmatrix}, \quad (116)$$

where the components  $\phi^+$ ,  $H$ ,  $\chi$  have vacuum expectation values zero. Expanding the potential (113) around the vacuum configuration in terms of the components yields a mass term for  $H$ , whereas  $\phi^+$ , and  $\chi$  are massless. Exploiting the invariance of the Lagrangian, the components  $\phi^+$ ,  $\chi$  can be eliminated by a suitable gauge transformation; this means that they are unphysical degrees of freedom (called Higgs ghosts or would-be Goldstone bosons). Choosing this particular gauge where  $\phi^+ = \chi = 0$ , denoted as the unitary gauge, the Higgs doublet field has the simple form

$$\Phi(x) = \frac{1}{\sqrt{2}} \begin{pmatrix} 0 \\ v + H(x) \end{pmatrix}, \quad (117)$$

and the potential (113) reads

$$V = \mu^2 H^2 + \frac{\mu^2}{v} H^3 + \frac{\mu^2}{4v^2} H^4 = \frac{M_H^2}{2} H^2 + \frac{M_H^2}{2v} H^3 + \frac{M_H^2}{8v^2} H^4. \quad (118)$$

The real field  $H(x)$  thus describes physical neutral scalar particles, the Higgs bosons, with mass

$$M_H = \mu\sqrt{2}, \quad (119)$$

as well as triple and quartic self interactions with couplings proportional to  $M_H^2$ . The couplings to the gauge fields follow from the kinetic term of (111) and give rise to trilinear  $HW$ ,  $HZZ$  and quadrilinear  $HHWW$ ,  $HHZZ$  vertices.

In order to solve the mass problem for the fermions, Yukawa interactions between the Higgs field and the fermion fields are introduced in addition to get the charged fermions massive. The gauge-invariant Yukawa term in the Lagrangian, for one family of leptons and quarks, is a compact expression in terms of the doublets  $L_L = (\nu_L, l_L)^T$ ,  $Q_L = (u_L, d_L)^T$  and the Higgs field  $\Phi$  and its charge-conjugate  $\Phi^c = i\sigma_2 \Phi = (\phi^{0*}, -\phi^-)^T$  with  $\phi^-$  as the adjoint of  $\phi^+$ ,

$$\mathcal{L}_Y = -G_l \bar{L}_L \Phi l_R - G_d \bar{Q}_L \Phi d_R - G_u \bar{Q}_L \Phi^c u_R + h.c. \quad (120)$$

It reads explicitly in terms of the Higgs field components (116)

$$\begin{aligned} \mathcal{L}_Y = & -G_l (\bar{\nu}_L \phi^+ l_R + \bar{l}_R \phi^- \nu_L + \bar{l}_L \phi^0 l_R + \bar{l}_R \phi^{0*} l_L) \\ & - G_d (\bar{u}_L \phi^+ d_R + \bar{d}_R \phi^- u_L + \bar{d}_L \phi^0 d_R + \bar{d}_R \phi^{0*} d_L) \\ & - G_u (-\bar{u}_R \phi^+ d_L - \bar{d}_L \phi^- u_R + \bar{u}_R \phi^0 u_L + \bar{u}_L \phi^{0*} u_R). \end{aligned} \quad (121)$$

The fermion mass terms follow from the  $v$  part of  $\phi^0$  in (117), relating the individual Yukawa coupling constants  $G_{l,d,u}$  to the masses of the charged fermions by

$$m_f = G_f \frac{v}{\sqrt{2}}. \quad (122)$$

In the unitary gauge (117) the Yukawa Lagrangian becomes particularly simple:

$$\mathcal{L}_Y = - \sum_f m_f \bar{\psi}_f \psi_f - \sum_f \frac{m_f}{v} \bar{\psi}_f \psi_f H. \quad (123)$$

As a remnant of this mechanism, Yukawa interactions between the massive fermions and the physical Higgs field occur with coupling constants proportional to the fermion masses.

In the realistic case of three generations, one has to take into account flavour mixing in the quark sector (in the lepton sector, lepton number is conserved and flavour mixing is absent in the minimal model). Quark-family mixing is induced by Yukawa interactions with the Higgs field as before, but the Yukawa couplings are now matrices in generation space with complex entries,  $G_u = (G_{ij}^u)$ ,  $G_d = (G_{ij}^d)$ ,

and the generalization of (121) for the quark sector reads as follows, with the notation  $Q_L^i = (u_L^i, d_L^i)^T$  for the three left-handed doublets [ $u^i = u, c, t$  and  $d^i = d, s, b$ ]:

$$\mathcal{L}_Y^{\text{quarks}} = -G_{ij}^d \bar{Q}_L^i \Phi d_R^j - G_{ij}^u \bar{Q}_L^i \Phi^c u_R^j + h.c. \quad (124)$$

The mass term is obtained from replacing  $\Phi$  by its vacuum configuration,  $\Phi \rightarrow \langle \Phi \rangle$  from (115),

$$- \frac{v}{\sqrt{2}} G_{ij}^d \bar{d}_L^i d_R^j - \frac{v}{\sqrt{2}} G_{ij}^u \bar{u}_L^i u_R^j + h.c. \quad (125)$$

This bilinear term in the quark fields can be diagonalized with the help of four unitary matrices  $V_{L,R}^q$  ( $q = u, d$ ), yielding the mass eigenstates

$$\tilde{u}_{L,R}^i = (V_{L,R}^u)_{ik} u_{L,R}^k, \quad \tilde{d}_{L,R}^i = (V_{L,R}^d)_{ik} d_{L,R}^k, \quad (126)$$

as well as the  $u$ - and  $d$ -type quark masses as diagonal mass matrices,

$$\text{diag}(m_q) = \frac{v}{\sqrt{2}} V_L^q G_q V_R^{q\dagger}, \quad q = u, d. \quad (127)$$

Introducing the mass eigenstates in the fermion–gauge Lagrangian (109) does not change the flavour-diagonal terms, i.e., the kinetic term and the interaction terms with the neutral gauge bosons, because of the unitarity of the transformations (126). Also the Yukawa interaction of the physical Higgs field with the quarks, when expressed in terms of the quark masses and the mass eigenstates, retains its structure as given in (123). The only modification occurs in the flavour-changing quark interaction with the charged vector bosons in (109) where the insertion of the mass eigenstates for the left-handed quark fields introduces the unitary CKM matrix,

$$V_L^u V_L^{d\dagger} \equiv V_{\text{CKM}}. \quad (128)$$

Given the constraints from unitarity,  $V_{\text{CKM}}$  has four independent physical parameters, three real angles and one complex phase.

For neutrino masses zero, no generation mixing in the lepton sector occurs. It is, however, possible to augment the Standard Model by introducing also right-handed neutrinos and neutrino mass terms in analogy to those of the  $u$ -type quark sector allowing for lepton-flavour mixing as well. The general treatment of lepton masses and mixing would, however, go beyond the scope of these lectures (for a discussion of neutrino masses see Ref. [7]).

**Physical fields and parameters.** The gauge invariant Higgs–gauge field interaction in the kinetic part of (111) gives rise to mass terms for the vector bosons in the non-diagonal form

$$\frac{1}{2} \left( \frac{g_2}{2} v \right)^2 (W_1^2 + W_2^2) + \frac{1}{2} \left( \frac{v}{2} \right)^2 (W_\mu^3, B_\mu) \begin{pmatrix} g_2^2 & g_1 g_2 \\ g_1 g_2 & g_1^2 \end{pmatrix} \begin{pmatrix} W^{3,\mu} \\ B^\mu \end{pmatrix}. \quad (129)$$

The physical content becomes transparent by performing a transformation from the fields  $W_\mu^a, B_\mu$  (in terms of which the symmetry is manifest) to the physical fields

$$W_\mu^\pm = \frac{1}{\sqrt{2}} (W_\mu^1 \mp i W_\mu^2) \quad (130)$$

and

$$\begin{pmatrix} Z_\mu \\ A_\mu \end{pmatrix} = \begin{pmatrix} \cos \theta_W & \sin \theta_W \\ -\sin \theta_W & \cos \theta_W \end{pmatrix} \begin{pmatrix} W_\mu^3 \\ B_\mu \end{pmatrix}. \quad (131)$$

In these fields the mass term (129) is diagonal and has the form

$$M_W^2 W_\mu^+ W^{-\mu} + \frac{1}{2} (A_\mu, Z_\mu) \begin{pmatrix} 0 & 0 \\ 0 & M_Z^2 \end{pmatrix} \begin{pmatrix} A^\mu \\ Z^\mu \end{pmatrix} \quad (132)$$

with

$$M_W = \frac{1}{2} g_2 v, \quad M_Z = \frac{1}{2} \sqrt{g_1^2 + g_2^2} v. \quad (133)$$

The mixing angle in the rotation (131) is determined by

$$\cos \theta_W = \frac{g_2}{\sqrt{g_1^2 + g_2^2}} = \frac{M_W}{M_Z}. \quad (134)$$

Inserting the rotation (131) into the interaction part of  $\mathcal{L}_F$  in (109) and identifying  $A_\mu$  with the photon field which couples via the electric charge  $e$  to the electron,  $e$  can be expressed in terms of the gauge couplings in the following way:

$$e = \frac{g_1 g_2}{\sqrt{g_1^2 + g_2^2}}, \quad \text{or} \quad g_2 = \frac{e}{\sin \theta_W}, \quad g_1 = \frac{e}{\cos \theta_W}. \quad (135)$$

The relations above allow us to replace the original set of parameters  $g_2, g_1, \lambda, \mu^2, G_f$  by the equivalent set of more physical parameters  $e, M_W, M_Z, M_H, m_f, V_{\text{CKM}}$ , where each of them can (in principle) be measured directly in a suitable experiment. At present, all parameters are empirically known with the exception of the mass of the Higgs boson,  $M_H$ .

**Gauge interactions.** The fermion–gauge interactions are part of the fermion–gauge Lagrangian (109); expressed in the physical field and parameters, they appear as interactions of the electromagnetic current  $J_{\text{em}}^\mu$ , the weak neutral current  $J_{\text{NC}}^\mu$ , and the weak charged current  $J_{\text{CC}}^\mu$  with the corresponding vector fields,

$$\mathcal{L}_{\text{FG}} = J_{\text{em}}^\mu A_\mu + J_{\text{NC}}^\mu Z_\mu + J_{\text{CC}}^\mu W_\mu^+ + J_{\text{CC}}^{\mu \dagger} W_\mu^-, \quad (136)$$

with the currents

$$\begin{aligned} J_{\text{em}}^\mu &= -e \sum_{f=l,q} Q_f \bar{\psi}_f \gamma^\mu \psi_f, \\ J_{\text{NC}}^\mu &= \frac{g_2}{2 \cos \theta_W} \sum_{f=l,q} \bar{\psi}_f (v_f \gamma^\mu - a_f \gamma^\mu \gamma_5) \psi_f, \\ J_{\text{CC}}^\mu &= \frac{g_2}{\sqrt{2}} \left( \sum_{i=1,2,3} \bar{\nu}^i \gamma^\mu \frac{1 - \gamma_5}{2} e^i + \sum_{i,j=1,2,3} \bar{u}^i \gamma^\mu \frac{1 - \gamma_5}{2} V_{ij} d^j \right). \end{aligned} \quad (137)$$

In analogy to the notation for the quark fields in (124), the lepton families are labelled by  $e^i = e, \mu, \tau$  for the charged leptons and  $\nu^i = \nu_e, \nu_\mu, \nu_\tau$  for the corresponding neutrinos. The neutral current coupling constants in (137) are determined by the charge  $Q_f$  and isospin  $I_3^f$  of  $f_L$ ,

$$\begin{aligned} v_f &= I_3^f - 2Q_f \sin^2 \theta_W, \\ a_f &= I_3^f. \end{aligned} \quad (138)$$

The quantities  $V_{ij}$  in the charged current are the elements of the CKM matrix (128), which describes family mixing in the quark sector. Owing to the unitarity of  $V_{\text{CKM}}$ , the electromagnetic and the weak neutral current interaction are flavour-diagonal. Hence, flavour-changing processes resulting from neutral

current interactions can only occur at higher order; they are mediated by loop contributions and are consequently suppressed by additional powers of the fine-structure constant  $\alpha$ .

Besides the fermion–gauge interactions, the non-Abelian structure of the gauge group induces self-interactions between the vector bosons. These gauge self-interactions are contained in the pure gauge-field part (105) of the Lagrangian. Expressing the fields  $W_\mu^a$  and  $B_\mu$  in (104) resp. (105) by the physical fields  $A_\mu$ ,  $Z_\mu$ , and  $W_\mu^\pm$  yields a self-interaction term with triple and quartic couplings, which by use of the notation  $F_{\mu\nu} = \partial_\mu A_\nu - \partial_\nu A_\mu$ ,  $Z_{\mu\nu} = \partial_\mu Z_\nu - \partial_\nu Z_\mu$  can be written in the following way,

$$\begin{aligned} \mathcal{L}_{G,\text{self}} = & e [(\partial_\mu W_\nu^+ - \partial_\nu W_\mu^+) W^{-\mu} A^\nu + W_\mu^+ W_\nu^- F^{\mu\nu} + h.c.] \\ & + e \cot \theta_W [(\partial_\mu W_\nu^+ - \partial_\nu W_\mu^+) W^{-\mu} Z^\nu + W_\mu^+ W_\nu^- Z^{\mu\nu} + h.c.] \\ & - e^2 / (4 \sin^2 \theta_W) [(W_\mu^- W_\nu^+ - W_\nu^- W_\mu^+) W_\mu^+ W_\nu^- + h.c.] \\ & - e^2 / 4 (W_\mu^+ A_\nu - W_\nu^+ A_\mu) (W^{-\mu} A^\nu - W^{-\nu} A^\mu) \\ & - e^2 / 4 \cot^2 \theta_W (W_\mu^+ Z_\nu - W_\nu^+ Z_\mu) (W^{-\mu} Z^\nu - W^{-\nu} Z^\mu) \\ & + e^2 / 2 \cot \theta_W (W_\mu^+ A_\nu - W_\nu^+ A_\mu) (W^{-\mu} Z^\nu - W^{-\nu} Z^\mu) + h.c. \end{aligned} \quad (139)$$

In the Standard Model the coefficients of the self-couplings are exclusively determined by the gauge symmetry. Deviations from these values could only be of non-standard origin, e.g., as remnants from new physics at some higher mass scale.

## 7 Electroweak parameters and precision observables

Before predictions can be made from the electroweak theory, the input parameters have to be determined from experiments. As specified in the previous section, a convenient choice is the set of physical parameters given by the particle masses and the electromagnetic coupling  $e$ , which is commonly expressed in terms of the fine-structure constant  $\alpha = e^2/4\pi$ , a very precisely known low-energy parameter. Apart from the flavour sector with the fermion masses and mixing angles, only three independent quantities are required for fixing the input for the gauge sector and the fermion–gauge interactions. Conveniently, the vector-boson masses  $M_{W,Z}$  and  $\alpha$  are selected (equivalent to  $g_1, g_2, v$ ).

### 7.1 Lowest-order relations

In the unitary gauge (117), the propagators of the  $W$  and  $Z$  have the form as given in (31) for massive vector fields, but with a finite width  $\Gamma$  according to a Breit–Wigner shape for unstable particles,

$$i D_{\rho\nu}(k) = \frac{i}{k^2 - M_{W,Z}^2 + i M_{W,Z} \Gamma_{W,Z}} \left( -g_{\nu\rho} + \frac{k_\nu k_\rho}{M_{W,Z}^2} \right). \quad (140)$$

In processes with light fermions as external particles, the  $k_\rho k_\nu$  terms are negligible since they are suppressed by powers of  $m_f/M_{W,Z}$ . The widths become important around the poles, i.e., when the vector bosons can be produced on-shell, like in  $e^+e^-$  annihilation or in Drell–Yan processes in hadron–hadron collisions.

A very precisely measured low-energy parameter is the Fermi constant  $G_F$ , which is the effective 4-fermion coupling constant in the Fermi model, obtained from the muon lifetime to be [8]  $G_F = 1.16637(1) \cdot 10^{-5} \text{ GeV}^{-2}$ .

Muon decay is described in the Standard Model in lowest order by exchange of a  $W$  boson between the fermionic charged currents, as shown in Fig. 4. Consistency of the Standard Model at the muon mass scale much smaller than  $M_W$ , where the momentum in the  $W$  propagator can be neglected, with the Fermi model requires the identification

$$\frac{G_F}{\sqrt{2}} = \frac{g_2^2}{8M_W^2} = \frac{e^2}{8 \sin^2 \theta_W M_W^2} = \frac{e^2}{8 \sin^2 \theta_W \cos^2 \theta_W M_Z^2}, \quad (141)$$

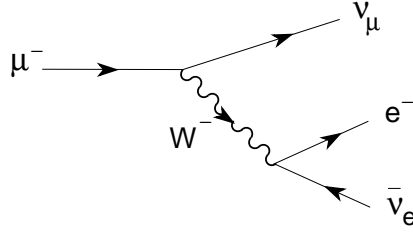


**Fig. 4:** Muon decay lowest-order amplitude in the Standard Model

which allows us to relate the vector boson masses to the parameters  $\alpha$ ,  $G_F$ ,  $\sin^2 \theta_W$  and to establish also the  $M_W$ – $M_Z$  interdependence in terms of precise low-energy parameters,

$$M_W^2 \left( 1 - \frac{M_W^2}{M_Z^2} \right) = \frac{\pi\alpha}{\sqrt{2}G_F} \equiv A^2, \quad A = 37.2805 \text{ GeV}. \quad (142)$$

Moreover, it yields the vacuum expectation value expressed in terms of the Fermi constant, also denoted as the Fermi scale,

$$v = (\sqrt{2}G_F)^{-\frac{1}{2}} = 246 \text{ GeV}. \quad (143)$$

The relation (141) can be further exploited to express the normalization of the NC couplings in (137) in terms of the Fermi constant,

$$\frac{g_2}{2 \cos \theta_W} = (\sqrt{2}G_F M_Z^2)^{\frac{1}{2}}. \quad (144)$$

In this way, the NC vector and axial vector coupling constants of each fermion species to the  $Z$  are determined and can be used to calculate the variety of observables at the  $Z$  resonance, like  $Z$  width and partial widths,

$$\Gamma_Z = \sum_f \Gamma(Z \rightarrow f\bar{f}), \quad \Gamma(Z \rightarrow f\bar{f}) = \frac{M_Z}{12\pi} (v_f^2 + a_f^2) \quad (145)$$

and a series of asymmetries, such as forward–backward asymmetries from the cross sections integrated over the forward ( $\sigma_F$ ) and the backward ( $\sigma_B$ ) hemisphere,

$$A_{FB} = \frac{\sigma_F - \sigma_B}{\sigma_F + \sigma_B} = \frac{3}{4} A_e A_f, \quad (146)$$

and the left–right asymmetry from the cross sections  $\sigma_{L,R}$  for left- and right-handed polarized electrons,

$$A_{LR} = \frac{\sigma_L - \sigma_R}{\sigma_L + \sigma_R} = A_e, \quad (147)$$

all of them being determined by the ratios

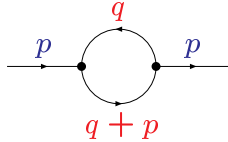
$$A_f = \frac{2v_f a_f}{v_f^2 + a_f^2} \quad (148)$$

with the coupling constants  $v_f, a_f$  given in (138). The asymmetries are particularly sensitive to the electroweak mixing angle  $\sin^2 \theta_W$ .

## 7.2 Higher-order contributions

### 7.2.1 Loop calculations

These lowest-order relations given above, however, turn out to be significantly insufficient when confronted with the experimental data, which have been measured with extraordinary accuracy during the LEP and Tevatron era and require the inclusion of terms beyond the lowest order in perturbation theory. The high experimental precision makes the observables sensitive to the quantum structure of the theory which appears in terms of higher-order contributions involving diagrams with closed loops in the Feynman-graph expansion. These loop diagrams contain, in general, integrals that diverge for large integration momenta, for example in the self-energy diagrams for a propagator, typically



$$\int d^4q \frac{1}{(q^2 - m_1^2) [(q+p)^2 - m_2^2]} \sim \int \frac{d^4q}{q^4} \rightarrow \infty. \quad (149)$$

Nevertheless, the relations between physical observables result as finite and testable predictions, owing to the virtue of renormalizability. The possibility to perform such higher-order calculations is based on the formulation of the Standard Model as a renormalizable quantum field theory preserving its predictive power also beyond the tree level. Renormalizability is thereby guaranteed by local gauge invariance of the basic Lagrangian.

The first step to deal with the divergent integrals is a method for regularization, which is a procedure to redefine the integrals in such a way that they become finite and mathematically well-defined objects. The widely used regularization procedure for gauge theories is that of dimensional regularization which is Lorentz and gauge invariant: replace the dimension 4 by a lower dimension  $D$  where the integrals are convergent (see Appendix C),

$$\int d^4q \rightarrow \mu^{4-D} \int d^Dq. \quad (150)$$

Thereby, an (arbitrary) mass parameter  $\mu$  is introduced to maintain the mass dimensions of the integrals.

The divergences manifest themselves in terms of poles in the dimension  $\sim 1/(4-D)$ . In renormalizable theories these divergences can be absorbed in the basic parameters of the Lagrangian, like masses and coupling constants. Formally this procedure, called renormalization, is done by introducing a counter term for each parameter [for example  $m^2 \rightarrow m^2 + \delta m^2$  for a mass parameter  $m$ ] which cancels the singularities; the finite part of the counter terms, however, is not a priori fixed and has to be defined by a renormalization scheme. The selection of a renormalization scheme defines the physical meaning of each parameter and its relation to measurable quantities. These relations are then independent of  $D$  and thus one can set  $D \rightarrow 4$ .

In pure QCD, considering quarks as massless, the only basic parameter is the strong coupling constant  $\alpha_s$ . Since there is no intrinsic mass scale, the frequently used scheme is the  $\overline{MS}$  scheme [9], where the counter term for  $\alpha_s$  consists only of the singular pole part (together with a universal numerical constant). The coupling is then defined for the chosen mass scale  $\mu$  in (150), the renormalization scale, and thus becomes a scale-dependent quantity, the running coupling constant  $\alpha_s(\mu)$  (see Ref. [6]).

The Lagrangian of the electroweak Standard Model involves quite a few free parameters which are not fixed by the theory but have to be taken from experiment. In QED and in the electroweak theory, classical Thomson scattering and the particle masses set natural scales where the parameters can be defined. A distinguished choice for the basic parameters is thus given by the fundamental charge  $e$  and

the masses of the particles,  $M_Z, M_W, M_H, m_f$ , and a common choice for the renormalization is the on-shell scheme: the mass parameters coincide with the poles of corresponding propagators (pole masses), and the charge  $e$  is defined in the classical limit. The on-shell scheme hence defines the counter terms in the following way (see, e.g., Ref. [10] for details):

- The mass counter term  $\delta m^2$ , for any free mass parameter  $m$ , is determined by the condition

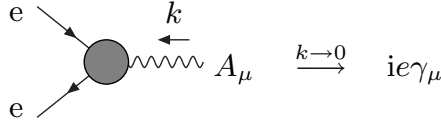
$$\delta m^2 = \Sigma(m^2), \quad (151)$$

where  $\Sigma$  is the self-energy of the corresponding particle, schematically depicted in (149) and yielding a dressed propagator

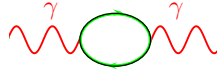
$$\frac{i}{p^2 - (m^2 + \delta m^2) + \Sigma(p^2)}, \quad (152)$$

which by mass renormalization now includes also the mass counterterm. The condition (151) ensures that  $m^2$  still remains the pole of the propagator.<sup>1</sup>

- The counter term  $\delta e$  for the electric charge,  $e \rightarrow e + \delta e$ , is determined by the requirement that  $e$  be the electron–photon coupling in the classical limit, i.e., for the electron–photon vertex for real photons,  $k^2 = 0$ , and for low photon energy,



$\delta e$  is essentially given by the charged-light-fermion contribution to the photon vacuum polarization at zero momentum,  $\Pi^\gamma(0)$ ,

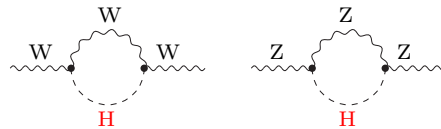


which has a finite part  $\Delta\alpha = \Pi^\gamma(0) - \Pi^\gamma(M_Z^2)$  yielding a shift of  $\Delta\alpha \simeq 0.06$  in the electromagnetic fine-structure constant  $\alpha \rightarrow \alpha(1 + \Delta\alpha)$ .  $\Delta\alpha$  can be resummed according to the renormalization group, accommodating all the leading logarithms of the type  $\alpha^n \log^n(M_Z/m_f)$  from the light fermions. The result is an effective fine-structure constant at the  $Z$  mass scale

$$\alpha(M_Z^2) = \frac{\alpha}{1 - \Delta\alpha} \simeq \frac{1}{129}. \quad (153)$$

It corresponds to a resummation of the iterated 1-loop vacuum polarization from the light fermions to all orders.  $\Delta\alpha$  is an input of crucial importance because of its universality and remarkable numerical size [11, 12].

The loop contributions to the electroweak observables contain all particles of the Standard Model spectrum, in particular also the Higgs boson, as, for example, in the vector-boson self-energies



The higher-order terms thus induce a dependence of the observables on the Higgs-boson mass  $M_H$ , which by means of precision measurements becomes indirectly accessible, although still unknown from direct searches. For more details see Ref. [13] and references therein.

<sup>1</sup>In the  $\overline{MS}$  scheme,  $\delta m^2$  only absorbs the divergent part of  $\Sigma(m^2)$ . The remaining finite part depends on the renormalization scale  $\mu$ , and in that scheme the mass becomes a  $\mu$ -dependent parameter, the running mass  $m(\mu)$ , which is different from the pole mass.

### 7.2.2 Vector boson masses and Fermi constant

The implementation of higher-order terms can be done in a compact way for the  $W$ - $Z$  mass correlation,

$$M_W^2 \left( 1 - \frac{M_W^2}{M_Z^2} \right) = \frac{A^2}{1 - \Delta r}. \quad (154)$$

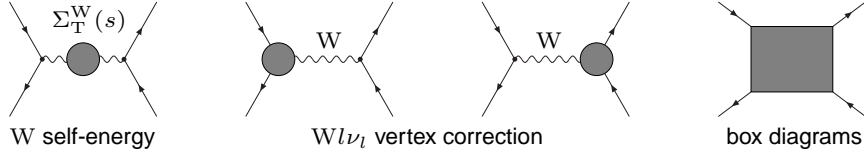


**Fig. 5:** Loop contributions to the muon decay amplitude

Therein, the contributions from the loop diagrams to the muon decay amplitude, schematically depicted in Fig. 5, are summarized by the quantity  $\Delta r = \Delta r(m_t, M_H)$ , which at one-loop order depends logarithmically on the Higgs-boson mass and quadratically on the top-quark mass. The calculation of  $\Delta r$  is complete at the two-loop level [14] and comprises the leading terms also at the three- and four-loop level [15]. The prediction of  $M_W$  from (154) is shown in Fig. 6 [16].

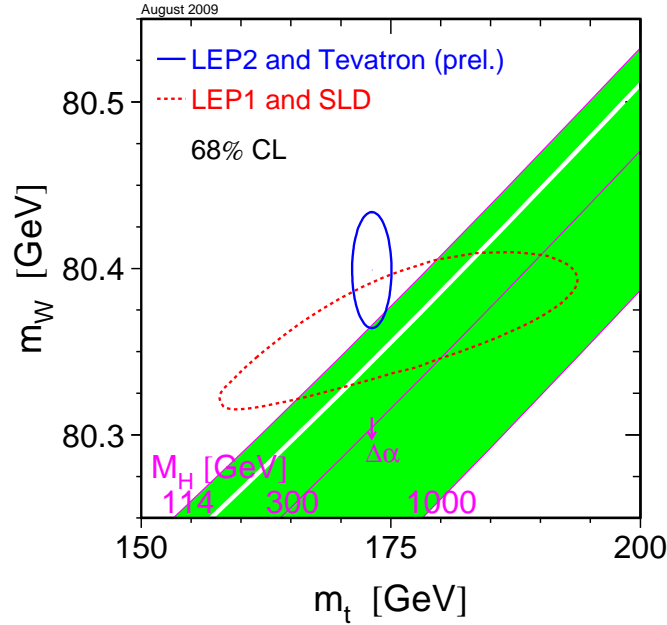


**Fig. 6:** Standard Model predictions for the dependence of  $M_W$  on the masses of the top quark and Higgs boson

### 7.2.3 Observables at the Z resonance

The NC couplings dressed by higher-order terms can also be written in a compact way, replacing the lowest-order couplings (138) by effective couplings [13],

$$g_V^f = \sqrt{\rho_f} (I_3^f - 2Q_f \sin^2 \theta_{\text{eff}}^f), \quad g_A^f = \sqrt{\rho_f} I_3^f, \quad (155)$$

which comprise the higher-order contributions in terms of the form factor  $\rho_f(m_t, M_H)$  and the effective mixing angle  $\sin^2 \theta_{\text{eff}}^f(m_t, M_H)$ , being now a fermion-type dependent quantity. Again, their dependence

on  $m_t$  is quadratic, whereas they depend on  $M_H$  only logarithmically. Nevertheless, the leptonic effective mixing angle is one of the most constraining observables for the mass of the Higgs boson, as shown in Fig. 7 [16]. Like for  $\Delta r$ , the calculation is complete at the two-loop level [17] and supplemented by 3- and 4-loop leading terms [15].

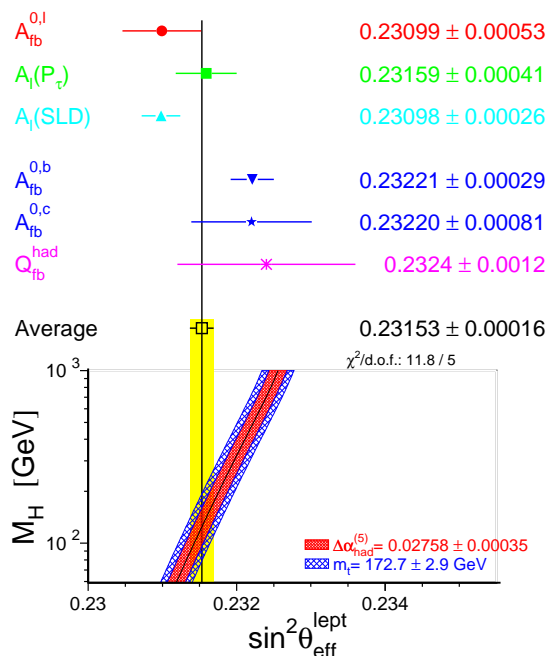


**Fig. 7:** Standard Model predictions for the dependence of  $\sin^2 \theta_{\text{eff}}^{\text{lept}}$  on the mass of the Higgs boson and the experimental  $1\sigma$ -range from averaged measurements done at LEP and SLC

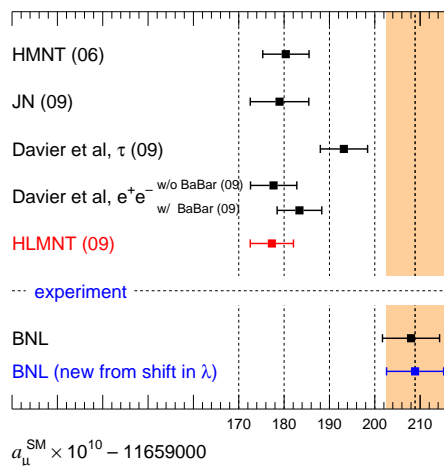


**Fig. 8:** Measurements and Standard Model predictions for  $a_\mu = (g_\mu - 2)/2$

### 7.2.4 Muon magnetic moment

The anomalous magnetic moment of the muon

$$a_\mu = \frac{g_\mu - 2}{2} \quad (156)$$

provides a precision test at low energies. The experimental result of E 821 at Brookhaven National Laboratory [18] has reached a substantial improvement in accuracy. It shows a deviation from the Standard Model prediction by 3–4 standard deviations depending on the evaluation of the hadronic vacuum polarization from data based on  $e^+e^-$  annihilation as shown in Fig. 8 [12]. For a recent review see Ref. [19].

### 7.3 The vector-boson self-interaction

The success of the Standard Model in the correct description of the electroweak precision observables is simultaneously an indirect confirmation of the Yang–Mills structure of the gauge boson self-interaction. For conclusive confirmations direct experimental investigation is required. At LEP 2 (and higher energies), pair production of on-shell  $W$  bosons allows direct experimental tests of the trilinear vector boson self-couplings and precise  $M_W$  measurements. From LEP 2, an error of 33 MeV in  $M_W$  has been reached. Further improvements have been obtained from the Tevatron with currently 31 MeV uncertainty, yielding the world average for the  $W$  mass  $M_W = 80.399 \pm 0.023$  GeV [16].

Pair production of  $W$  bosons in the Standard Model is described by the amplitude based on the Feynman graphs in Fig. 9 (in Born approximation) and higher-order contributions [20].

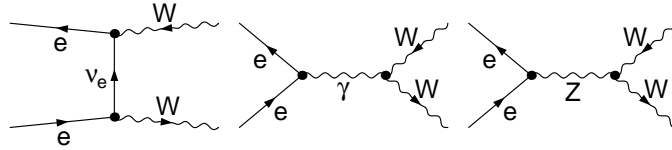


**Fig. 9:** Feynman graphs for  $e^+e^- \rightarrow W^+W^-$  in lowest order

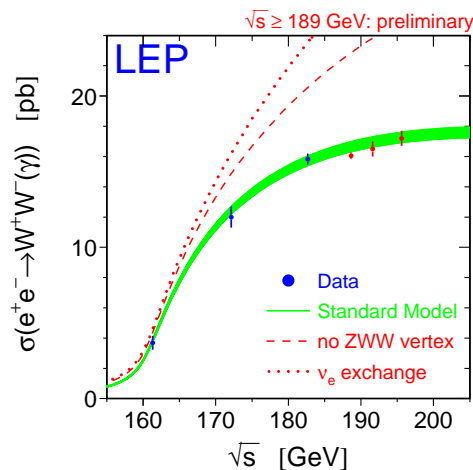


**Fig. 10:** Cross-section for  $e^+e^- \rightarrow W^+W^-$ , measured at LEP, and the Standard Model prediction

Besides the  $t$ -channel  $\nu$ -exchange diagram, which involves only the  $W$ -fermion coupling, the  $s$ -channel diagrams contain the triple gauge interaction between the vector bosons. The gauge self-interactions of

the vector bosons, as specified in (139) are essential for the high-energy behaviour of the production cross-section in accordance with the principle of unitarity. Deviations from these values spoil the high-energy behaviour of the cross-sections and would be visible at energies sufficiently above the production threshold. Measurements of the cross section for  $e^+e^- \rightarrow WW$  at LEP have confirmed the prediction of the Standard Model, as visualized in Fig. 10 [16].

#### 7.4 Global fits and Higgs boson mass bound

The  $Z$ -boson observables from LEP 1 and SLC together with  $M_W$  and the top-quark mass from LEP 2 and the Tevatron, constitute the set of high-energy quantities entering a global precision analysis. Global fits within the Standard Model to the electroweak precision data contain  $M_H$  as the only free parameter, yielding the results [16] shown in Fig. 11 and an upper limit to the Higgs mass at the 95% C.L. of  $M_H < 157$  GeV, including the present theoretical uncertainties of the Standard Model predictions visualized as the blue band [16] in Fig. 12. Taking into account the lower exclusion bound of 114 GeV for  $M_H$  from the direct searches via renormalizing the probability shifts the 95% C.L. upper bound to 186 GeV [16]. For similar analyses see Ref. [21].

The anomalous magnetic moment of the muon is practically independent of the Higgs boson mass; hence its inclusion in the fit does not change the bound on  $M_H$ , but it reduces the goodness of the overall fit.

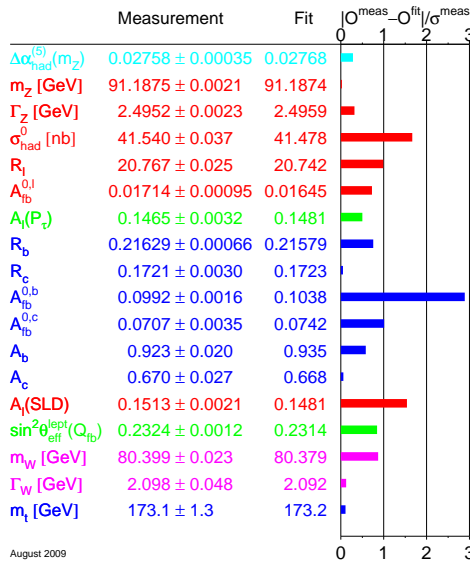
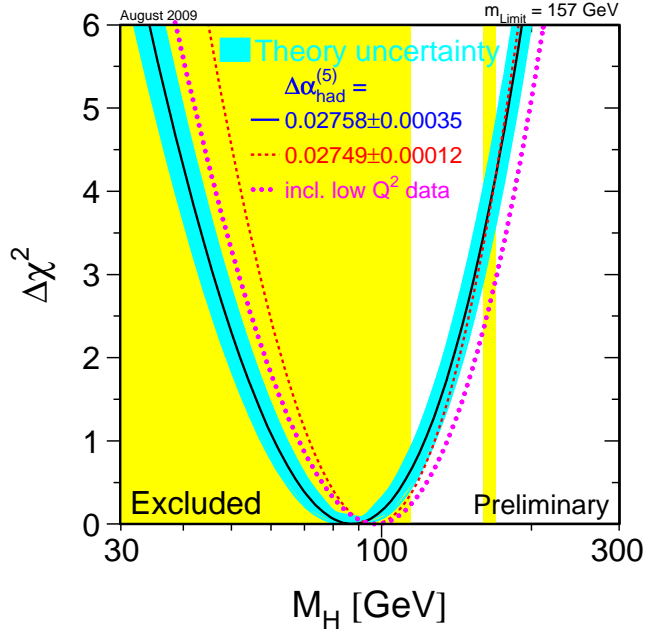


Fig. 11: Experimental measurements versus best-fit Standard Model values

#### 7.5 Perspectives for the LHC and the ILC

In the LHC era, further improved measurements of the electroweak parameters are expected, especially on the  $W$  mass and the mass of the top quark, as indicated in Table 2. The accuracy on the effective mixing angle, measurable from forward-backward asymmetries, will not exceed the one already obtained in  $e^+e^-$  collisions [22]. The detection of a Higgs boson would go along with a determination of its mass with an uncertainty of about 100 MeV.



**Fig. 12:**  $\chi^2$  distribution from a global electroweak fit to  $M_H$

At a future electron–positron collider, the International Linear Collider (ILC), the accuracy on  $M_W$  can be substantially improved via the scanning of the  $e^+e^- \rightarrow W^+W^-$  threshold region [23]. The GigaZ option, a high-luminosity  $Z$  factory, can provide in addition a significant reduction of the errors in the  $Z$  boson observables, in particular for the leptonic effective mixing angle, denoted by  $\sin^2 \theta_{\text{eff}}$ , with an error being an order of magnitude smaller than the present one. Moreover, the top-quark mass accuracy can also be considerably improved. The numbers are collected in Table 2.

An ultimate precision test of the Standard Model that would be possible in the future scenario with GigaZ [24] is illustrated in Fig. 13. The figure displays the 68% C.L. regions for  $M_W$  and  $\sin^2 \theta_{\text{eff}}$  expected from the LHC and ILC/GigaZ measurements; the small quadrangles denote the Standard Model predictions for a possible, experimentally determined, Higgs boson mass with the sides reflecting the parametric uncertainties from  $\Delta\alpha$  and the top-quark mass (for  $\Delta\alpha$ , a projected uncertainty of  $\delta\Delta\alpha = 5 \cdot 10^{-5}$  is assumed). If the Standard Model is correct, the two areas with the theory prediction and the future experimental results have to overlap. The central values chosen in Fig. 13 are just examples; the main message is the development of the uncertainties.

**Table 2:** Present experimental accuracies and expectations for future colliders

| Error for                    | Now     | Tevatron/LHC | LC   | GigaZ    |
|------------------------------|---------|--------------|------|----------|
| $M_W$ [MeV]                  | 23      | 15           | 10   | 7        |
| $\sin^2 \theta_{\text{eff}}$ | 0.00016 | 0.00021      |      | 0.000013 |
| $m_{\text{top}}$ [GeV]       | 1.3     | 1.0          | 0.2  | 0.13     |
| $M_{\text{Higgs}}$ [GeV]     | –       | 0.1          | 0.05 | 0.05     |

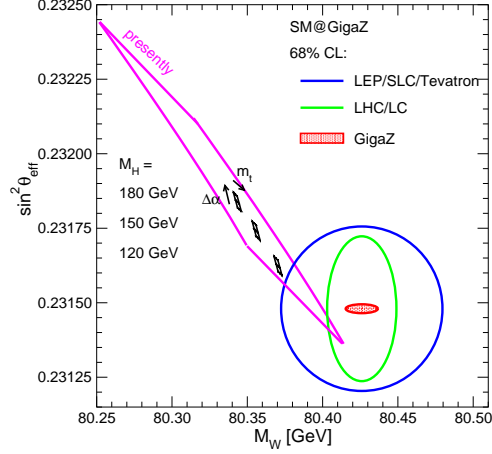


**Fig. 13:** Perspectives for Standard Model precision tests at future colliders

## 8 Higgs bosons

The minimal model with a single scalar doublet is the simplest way to implement the electroweak symmetry breaking. The Higgs potential of the Standard Model given in (113) involves two independent parameters  $\mu$  and  $\lambda$ , which can equivalently be replaced by the vacuum expectation value  $v$  and the Higgs boson mass  $M_H$ , as done in (118). The vacuum expectation value  $v$  is determined by the gauge sector, as explained in (129) and (143);  $M_H$  is independent and cannot be predicted but has to be taken from experiment. Thus in the Standard Model the mass  $M_H$  of the Higgs boson appears as the only free parameter that is still undetermined as yet. Expressed in terms of  $M_H$ , the Higgs part of the electroweak Lagrangian in the unitary gauge reads as follows:

$$\mathcal{L}_H = \frac{1}{2}(\partial_\mu H)(\partial^\mu H) - \frac{M_H^2}{2}H^2 - \frac{M_H^2}{2v}H^3 - \frac{M_H^2}{8v^2}H^4 + \left(M_W^2 W_\mu^+ W^{-\mu} + \frac{M_Z^2}{2}Z_\mu Z^\mu\right) \left(1 + \frac{H}{v}\right)^2 - \sum_f m_f \bar{\psi}_f \psi_f \left(1 + \frac{H}{v}\right), \quad (157)$$

involving interactions of the Higgs field with the massive fermions and gauge bosons, as well as Higgs self interactions proportional to  $M_H^2$ .

### 8.1 Empirical bounds

The existence of the Yukawa couplings and the couplings to the vector bosons  $W$  and  $Z$  is the basis for the experimental searches that have been performed until now at LEP and the Tevatron. At  $e^+e^-$  colliders, Higgs bosons can be produced by Higgs-strahlung from  $Z$  bosons and by vector boson fusion (mainly  $WW$ ) as displayed in Fig. 14.

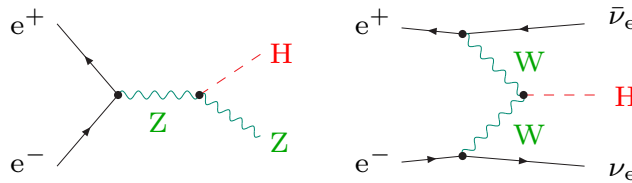


**Fig. 14:** Processes for Higgs boson production in  $e^+e^-$  collisions

At LEP energies, Higgs-strahlung is the relevant process. The lower limit at 95% C.L. resulting from the search at LEP is 114.4 GeV [8]. From searches at the Tevatron [25] (see Fig. 15 for various mechanisms) the mass range from 162 GeV to 166 GeV has been excluded (95% C.L.).

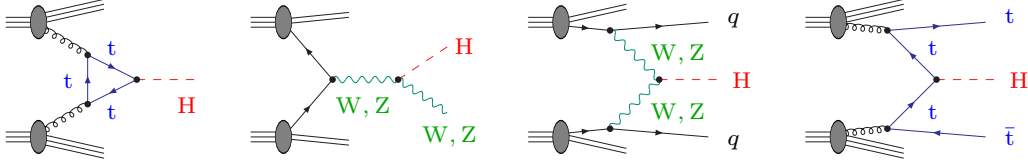


**Fig. 15:** Processes for Higgs boson production at hadron colliders

Indirect determinations of  $M_H$  from precision data yield an upper limit and have already been discussed in Section 7.4. As a general feature, it appears that the data prefer a light Higgs boson.

## 8.2 Theoretical bounds

There are also theoretical constraints on the Higgs mass from vacuum stability and absence of a Landau pole [26–28], and from lattice calculations [29, 30]. Explicit perturbative calculations of the decay width for  $H \rightarrow W^+W^-, ZZ$  in the large- $M_H$  limit,  $\Gamma(H \rightarrow VV) = K_V \cdot \Gamma^{(0)}(H \rightarrow VV)$  up to 2-loop order [31] have shown that the 2-loop contribution exceeds the 1-loop term in size (same sign) for  $M_H > 930$  GeV (Fig. 16 [32]). This result is confirmed by the calculation of the next-to-leading order correction in the  $1/N$  expansion, where the Higgs sector is treated as an  $O(N)$  symmetric  $\sigma$ -model [33]. A similar increase of the 2-loop perturbative contribution with  $M_H$  is observed for the fermionic decay width [34],  $\Gamma(H \rightarrow f\bar{f}) = K_f \cdot \Gamma^{(0)}(H \rightarrow f\bar{f})$ , but with opposite sign leading to a cancellation of the 1-loop correction for  $M_H \simeq 1100$  GeV (Fig. 16). The lattice result [30] for the bosonic Higgs decay in Fig. 16 for  $M_H = 727$  GeV is not far from the perturbative 2-loop result; the difference may at least partially be interpreted as missing higher-order terms.

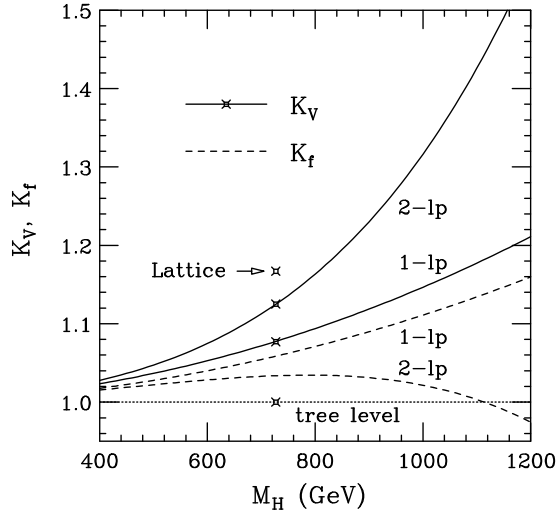
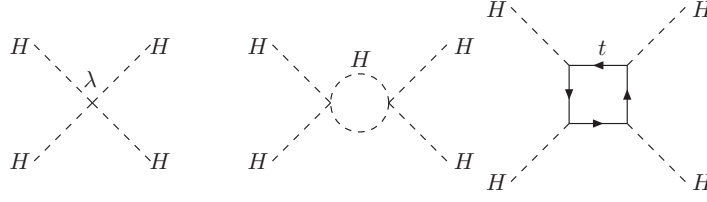


**Fig. 16:** Correction factors  $K_V, K_f$  from higher orders for the Higgs decay widths  $H \rightarrow VV$  ( $V = W, Z$ ) and  $H \rightarrow f\bar{f}$  in 1- and 2-loop order

The behaviour of the quartic Higgs self-coupling  $\lambda$ , as a function of a rising energy scale  $Q$ , follows from the renormalization group equation

$$\frac{d\lambda}{dt} = \frac{1}{16\pi^2} (12\lambda^2 + 6\lambda g_t^2 - 3g_t^4 + \dots), \quad t = \log \frac{Q^2}{v^2}, \quad (158)$$

with the  $\beta$ -function dominated by the contributions from  $\lambda$  and the top-quark Yukawa coupling  $g_t$  in the loop contributions to the quartic interactions,



Owing to the second diagram, the first term in (158),  $\lambda(Q)$  increases with  $Q$  and diverges at a critical scale, the Landau pole, which moves towards lower values for increasing mass  $M_H$ . The requirement of a perturbative, small coupling  $\lambda(Q)$  up to a scale  $\Lambda$  thus yields an upper bound for  $M_H$ . In order to avoid unphysical negative quartic couplings from the negative top-loop contribution, a lower bound on the Higgs mass is derived. In combination, the requirement that the Higgs coupling remain finite and positive up to a scale  $\Lambda$  yields constraints on the Higgs mass  $M_H$ , which have been evaluated at the 2-loop level [27, 28]. These bounds on  $M_H$  are shown in Fig. 17 [28] as a function of the cut-off scale  $\Lambda$  up to which the standard Higgs sector can be extrapolated. The allowed region is the area between the lower and the upper curves. The bands indicate the theoretical uncertainties associated with the solution of the renormalization group equations [28]. It is interesting to note that the indirect determination of the Higgs mass range from electroweak precision data via radiative corrections is compatible with a value of  $M_H$  where  $\Lambda$  can be extended up to the Planck scale.

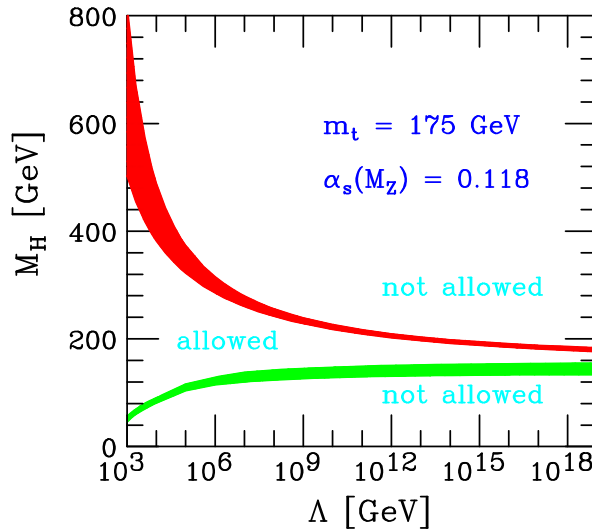


**Fig. 17:** Theoretical limits on the Higgs boson mass from the absence of a Landau pole and from vacuum stability

### 8.3 Future searches

For the coming experimental searches at the LHC, it is important to have precise and reliable predictions for the production and decay rates. Higgs bosons can be produced through various mechanisms at the partonic level. The main partonic processes for Higgs boson production are depicted in Fig. 15, and the corresponding production cross sections are shown in Fig. 18 [35]. The largest cross section arises from gluon–gluon fusion. The experimental signal, however, is determined by the product

$$\sigma(AB \rightarrow H) \cdot BR(H \rightarrow X) \quad (159)$$

of the production cross section  $\sigma(AB \rightarrow H)$  from initial-state partons  $A, B$  and the branching ratio  $BR(H \rightarrow X)$  for the decay of the Higgs boson into a specific final state  $X$  (see Fig. 19 for the branching

ratios [36]). A light Higgs boson, well below the  $WW$  threshold, decays predominantly into  $b\bar{b}$  quarks, owing to the largest Yukawa couplings in the kinematically allowed fermionic decay channels. This signal, however, is experimentally inaccessible because it is covered by a huge background of QCD-generated  $b$ -quark jets. Therefore, in the low mass range, the rare decay channel  $H \rightarrow \gamma\gamma$  has to be selected reducing the total number of events considerably, in spite of the large production cross section, and makes Higgs detection a cumbersome business. For larger masses,  $M_H \gtrsim 140$  GeV, the decay modes  $H \rightarrow WW, ZZ \rightarrow 4f$  make detection relatively easy. The vector-boson fusion channel (third diagram of Fig. 15) with subsequent leptonic decay  $H \rightarrow \tau^+\tau^-$  is a promising alternative.

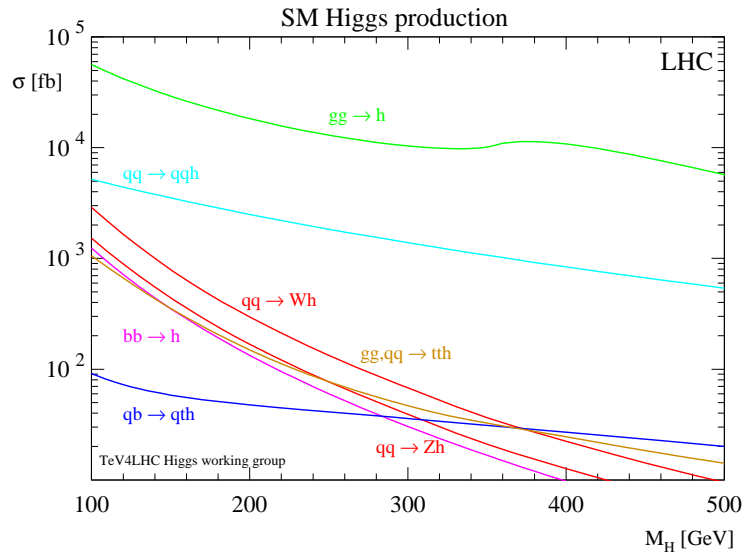


**Fig. 18:** Cross sections for Higgs boson production at the LHC

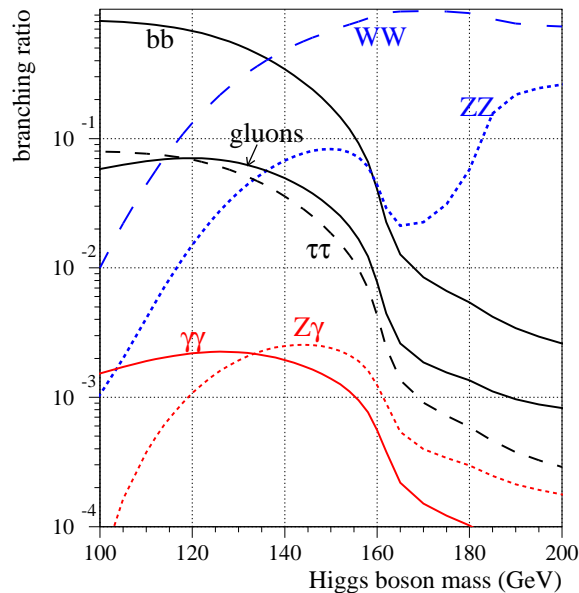


**Fig. 19:** Branching ratios for Higgs boson decays

For completeness we list the (lowest-order) expressions for the dominant Higgs decay rates into fermion and vector-boson pairs,

$$\begin{aligned}\Gamma(H \rightarrow f\bar{f}) &= N_C \frac{G_F M_H m_f^2}{4\pi\sqrt{2}} \sqrt{1 - \frac{4m_f^2}{M_H^2}} \quad \text{with } N_C = 3 \text{ for } f = q, \quad N_C = 1 \text{ for } f = \ell, \\ \Gamma(H \rightarrow VV) &= \frac{G_F M_H^3}{16\pi\sqrt{2}} R_V(x_V), \quad x_V = \frac{M_V^2}{M_H^2}, \quad (V = W, Z)\end{aligned}\quad (160)$$

with

$$R_Z = R(x_Z), \quad R_W = 2 R(x_W), \quad R(x) = \sqrt{1 - 4x} (1 - 4x + 12x^2). \quad (161)$$

As an exercise, these formulae can easily be derived from the  $Hff$  and  $HVV$  vertices in (157) with the help of the Feynman rules of Section 2 and the general expression for the width in (70).

#### 8.4 Supersymmetric Higgs bosons

Among the extensions of the Standard Model, the Minimal Supersymmetric Standard Model (MSSM) [37] is a theoretically favoured scenario as the most predictive framework beyond the Standard Model. A light Higgs boson, as indicated in the analysis of the electroweak precision data, would find a natural explanation by the structure of the Higgs potential. For a review on MSSM Higgs bosons see Ref. [38].

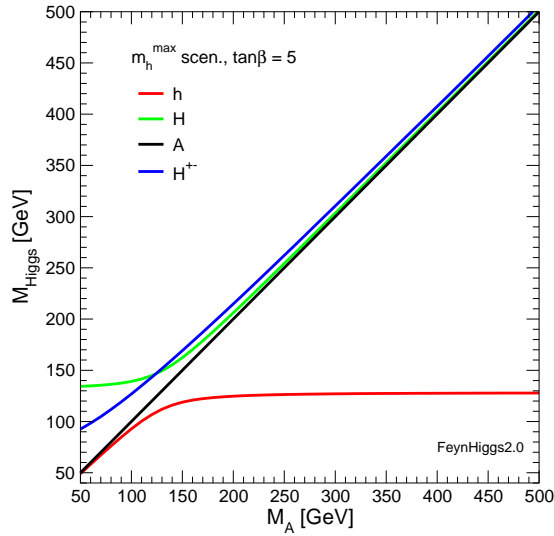


**Fig. 20:** Example of the Higgs boson mass spectrum in the MSSM

The five physical Higgs particles of the MSSM consist of two  $CP$ -even neutral bosons  $h^0, H^0$ , a  $CP$ -odd  $A^0$  boson, and a pair of charged Higgs particles  $H^\pm$ . At tree level, their masses are determined by the  $A^0$  boson mass,  $M_A$ , and the ratio of the two vacuum expectation values,  $v_2/v_1 = \tan \beta$ ,

$$\begin{aligned}M_{H^\pm}^2 &= M_A^2 + M_W^2, \\ M_{H^0, h^0}^2 &= \frac{1}{2} \left( M_A^2 + M_Z^2 \pm \sqrt{(M_A^2 + M_Z^2)^2 - 4M_Z^2 M_A^2 \cos^2 2\beta} \right).\end{aligned}\quad (162)$$

These relations are sizeably modified by higher-order contributions to the Higgs boson vacua and propagators. A typical example of a spectrum is shown in Fig. 20, based on the FEYNHIGGS code [39]. In particular the mass of the lightest Higgs boson  $h^0$  is substantially influenced by loop contributions; for

large  $M_A$ , the  $h^0$  particle behaves like the standard Higgs boson, but its mass is dependent on basically all the parameters of the model and hence yields another powerful precision observable. A definite prediction of the MSSM is thus the existence of a light Higgs boson with mass below  $\sim 140$  GeV. The detection of a light Higgs boson could be a significant hint for supersymmetry.

The structure of the MSSM as a renormalizable quantum field theory allows a similarly complete calculation of the electroweak precision observables as in the Standard Model in terms of one Higgs mass (usually taken as  $M_A$ ) and  $\tan\beta$ , together with the set of SUSY soft-breaking parameters fixing the chargino/neutralino and scalar fermion sectors [40]. For updated discussions of precision observables in the MSSM see Ref. [41].

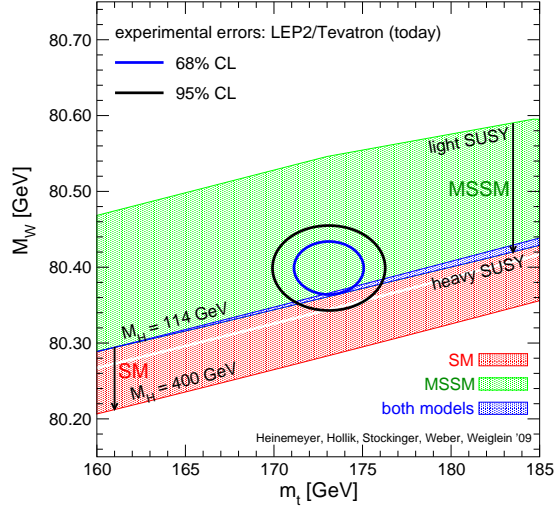


**Fig. 21:** The  $W$  mass range in the Standard Model (lower band) and in the MSSM (upper band) respecting bounds are from the non-observation of Higgs bosons and SUSY particles

As an example, Fig. 21 displays the range of predictions for  $M_W$  in the Standard Model and in the MSSM, together with the present experimental errors and the expectations for the LHC measurements. The MSSM prediction is in slightly better agreement with the present data for  $M_W$ , although not conclusive as yet. Future increase in the experimental accuracy, however, will become decisive for the separation between the models.

Especially for the muonic  $g - 2$ , the MSSM can significantly improve the agreement between theory and experiment: one-loop terms with relatively light scalar muons, sneutrinos, charginos and neutralinos,



in the mass range 200–600 GeV, together with a large value of  $\tan\beta$  can provide a positive contribution  $\Delta a_\mu$ , which can entirely explain the difference  $a_\mu^{\text{exp}} - a_\mu^{\text{SM}}$  (see Ref. [42] for a review).

The MSSM yields a comprehensive description of the precision data, in a similar way to the Standard Model. Global fits, varying the MSSM parameters, have been performed to all electroweak precision data [43] showing that the description within the MSSM is slightly better than in the Standard Model. This is mainly due to the improved agreement for  $a_\mu$ . The fits have been updated recently for the constrained MSSM (cMSSM), including also bounds from  $b \rightarrow s\gamma$  and from the cosmic relic density.

The  $\chi^2$ -distribution for the fit parameters can be shown [44] as a  $\chi^2$ -distribution for the lightest Higgs boson mass  $M_H$ , displayed in Fig. 22. The mass range  $M_h = 110_{-10}^{+9}$  GeV obtained from this fit is in much better agreement with the lower bound from the direct search than in the case of the Standard Model.

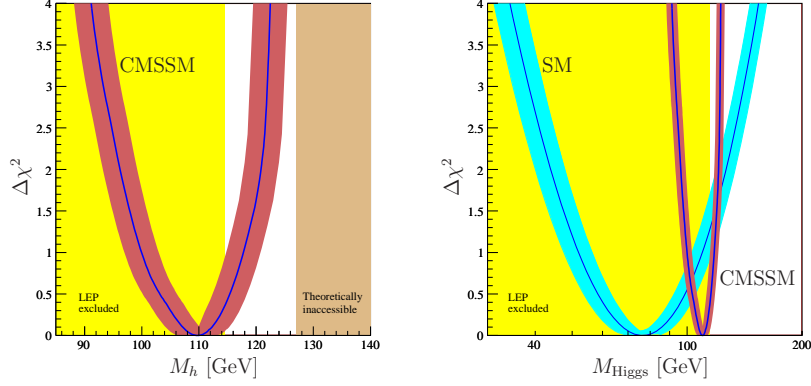


**Fig. 22:**  $\chi^2$ -distribution for cMSSM fits, expressed in terms of  $M_h$

## 9 Outlook

In spite of the success of the Standard Model in describing a large variety of phenomena, at a high level of accuracy on both the theoretical and the experimental side, there is a list of shortcomings that motivate the quest for physics beyond the Standard Model.

A rather direct augmentation is enforced by the need for accommodating massive neutrinos. The Standard Model in its strictly minimal version is incomplete with respect to a mass term for neutrinos. Neutrino mass terms can be added [7] without touching on the basic architecture of the Standard Model. Besides this rather immediate modification one is confronted, however, with a series of basic conceptual problems:

- the smallness of the electroweak scale  $v \sim 1/\sqrt{G_F}$  compared to the Planck scale  $M_{Pl} \sim 1/\sqrt{G_N}$  (the *hierarchy problem*) and the smallness of the Higgs boson mass of  $\mathcal{O}(v)$ , which is not protected against large quantum corrections of  $\mathcal{O}(M_{Pl})$ ;
- the large number of free parameters (gauge couplings, vacuum expectation value,  $M_H$ , fermion masses, CKM matrix elements), which are not predicted but have to be taken from experiments;
- the pattern that occurs in the arrangement of the fermion masses;
- the quantization of the electric charge, or the values of the hypercharge, respectively;
- the missing way to connect to gravity.

Moreover, there are also phenomenological shortcomings, like missing answers to the questions about

- the nature of dark matter that constitutes the largest fraction of matter in the Universe,
- the origin of the baryon asymmetry of the Universe.

The class of models based on supersymmetry, briefly addressed in the last subsection 8.4, can at least provide partial answers, e.g., for dark matter, the further unification of forces and hierarchy of mass scales, new sources of CP violation, and can be related to string theory as a candidate for a microscopic theory of gravity. The LHC experiments may soon shed light on our unanswered questions, or may also surprise us with answers to questions we did not ask.

## Appendices

### A Canonical commutation relations

The commutators between the canonically conjugate variables  $Q_j, P_k$  in quantum mechanics,

$$[Q_j, P_k] = i \delta_{jk}, \quad [Q_j, Q_k] = [P_j, P_k] = 0, \quad (\text{A.1})$$

are translated in quantum field theory to commutators for a (generic) field operator  $\phi(x) \equiv \phi(t, \vec{x})$  and its conjugate canonical momentum

$$\Pi(x) = \frac{\partial \mathcal{L}}{\partial(\partial_o \phi)} \quad (\text{A.2})$$

derived from the basic Lagrangian  $\mathcal{L}$  for the system. This procedure, known as canonical field quantization, is specified by the equal-time commutation relations, where the discrete indices  $j, k$  in (A.1) are replaced by the continuous indices  $\vec{x}, \vec{x}'$ :

$$[\phi(t, \vec{x}), \Pi(t, \vec{x}')] = i \delta^3(\vec{x} - \vec{x}'), \quad [\phi(t, \vec{x}), \phi(t, \vec{x}')] = [\Pi(t, \vec{x}), \Pi(t, \vec{x}')] = 0. \quad (\text{A.3})$$

For fermionic field variables  $\psi(x)$  the commutators have to be replaced by anti-commutators.

#### A.1 Scalar field

We illustrate the method of canonical quantization choosing the scalar field as a specific example. Starting from the Lagrangian (13) for a general, complex, free scalar field, we find the canonical field momenta via (A.2) to be

$$\begin{aligned} \frac{\partial \mathcal{L}}{\partial(\partial_o \phi)} &= \partial^0 \phi^\dagger = \dot{\phi}^\dagger = \Pi, \\ \frac{\partial \mathcal{L}}{\partial(\partial_o \phi^\dagger)} &= \partial^0 \phi = \dot{\phi} = \Pi^\dagger. \end{aligned} \quad (\text{A.4})$$

Accordingly, the canonical commutation relations are given by

$$\begin{aligned} [\phi(t, \vec{x}), \dot{\phi}^\dagger(t, \vec{x}')] &= i \delta^3(\vec{x} - \vec{x}'), \\ [\phi(t, \vec{x}), \phi(t, \vec{x}')] &= [\dot{\phi}(t, \vec{x}), \dot{\phi}(t, \vec{x}')] = 0. \end{aligned} \quad (\text{A.5})$$

These relations can equivalently be expressed in terms of the annihilation and creation operators  $a, b, a^\dagger, b^\dagger$  in the Fourier expansion of the scalar field  $\phi(x)$  in (14). They fulfil the following canonical commutation relations in momentum space and can be interpreted as those for a continuous set of quantized harmonic oscillators, labelled by  $\vec{k}$ , with frequencies  $\omega = k^0 = \sqrt{\vec{k}^2 + m^2}$  and with the relativistic normalization:

$$\begin{aligned} [a(k), a(k')] &= [b(k), b(k')] = 0, & [a^\dagger(k), a^\dagger(k')] &= [b^\dagger(k), b^\dagger(k')] = 0, \\ [a(k), a^\dagger(k')] &= 2k^0 \delta^3(\vec{k} - \vec{k}'), & [b(k), b^\dagger(k')] &= 2k^0 \delta^3(\vec{k} - \vec{k}'), \\ [a(k), b(k')] &= [a(k), b^\dagger(k')] = [a^\dagger(k), b(k')] &= [a^\dagger(k), b^\dagger(k')] = 0. \end{aligned} \quad (\text{A.6})$$

Since we do not make use of the formulation of quantization in space-time, but use instead the creation and annihilation operators, which are closer to the physical picture of particles and particle states, we list the commutators for the vector and spinor fields only in momentum space.

#### A.2 Vector field

For the vector field (25) the annihilation and creation operators  $a_\lambda, a_\lambda^\dagger$  carry helicity indices in addition to the momenta. Otherwise the commutation rules are analogous to the scalar case:

$$\begin{aligned} [a_\lambda(k), a_{\lambda'}(k')] &= [a_\lambda^\dagger(k), a_{\lambda'}^\dagger(k')] = 0, \\ [a_\lambda(k), a_{\lambda'}^\dagger(k')] &= 2k^0 \delta_{\lambda\lambda'} \delta^3(\vec{k} - \vec{k}'). \end{aligned} \quad (\text{A.7})$$

### A.3 Dirac field

The Dirac field (53) involves fermionic annihilation and creation operators  $c_\sigma, d_\sigma, c_\sigma^\dagger, d_\sigma^\dagger$  for each momentum  $\vec{k}$  and helicity  $\sigma$ . According to the antisymmetry of fermionic states, all commutators applying to bosonic states in the canonical quantization above have to be replaced by anti-commutators:

$$\begin{aligned} \{c_\sigma(k), c_{\sigma'}(k')\} &= \{c_\sigma^\dagger(k), c_{\sigma'}^\dagger(k')\} = 0, & \{c_\sigma(k), c_{\sigma'}^\dagger(k')\} &= 2k^0 \delta_{\sigma\sigma'} \delta^3(\vec{k} - \vec{k}'), \\ \{d_\sigma(k), d_{\sigma'}(k')\} &= \{d_\sigma^\dagger(k), d_{\sigma'}^\dagger(k')\} = 0, & \{d_\sigma(k), d_{\sigma'}^\dagger(k')\} &= 2k^0 \delta_{\sigma\sigma'} \delta^3(\vec{k} - \vec{k}'), \\ \{c_\sigma(k), d_{\sigma'}(k')\} &= \{c_\sigma^\dagger(k), d_{\sigma'}^\dagger(k')\} = \{c_\sigma(k), d_{\sigma'}^\dagger(k')\} = \{c_\sigma^\dagger(k), d_{\sigma'}(k')\} = 0. \end{aligned} \quad (\text{A.8})$$

### B Green functions and causality

We demonstrate, for the example of the scalar field, how the  $+i\epsilon$  prescription in the Fourier representation of the Feynman propagator leads to causal behaviour of particle/antiparticle propagation in space-time. Making use of the time-ordered product of any two field quantities  $A(x)$  and  $B(x)$ ,

$$TA(x)B(y) = \Theta(x^0 - y^0) A(x)B(y) + \Theta(y^0 - x^0) B(x)A(y), \quad (\text{B.1})$$

one can define the 2-point function for a (complex) scalar field  $\phi(x)$  in the following way:

$$\begin{aligned} \langle 0|T\phi(x)\phi^\dagger(y)|0\rangle &= \Theta(x^0 - y^0) \langle 0|\phi(x)\phi^\dagger(y)|0\rangle \\ &+ \Theta(y^0 - x^0) \langle 0|\phi^\dagger(y)\phi(x)|0\rangle. \end{aligned} \quad (\text{B.2})$$

Invoking the Fourier expansion for  $\phi$  and  $\phi^\dagger$  in terms of creation and annihilation operators (14), one can see that (B.2) describes particles created at time  $y^0$  and annihilated at time  $x^0$  if  $x^0 > y^0$ , and anti-particles created at time  $x^0$  and annihilated at time  $y^0$  if  $y^0 > x^0$ .

On the other hand, starting from the Fourier integral (17) and performing the  $k^0$  integration by means of a contour integral in the complex plane, one obtains the expression

$$\begin{aligned} D(x-y) &= \int \frac{d^4k}{(2\pi)^4} \frac{e^{-ik(x-y)}}{k^2 - m^2 + i\epsilon} \\ &= \int \frac{d^3k}{(2\pi)^3} e^{i\vec{k}(\vec{x}-\vec{y})} \int \frac{dk^0}{2\pi} \frac{e^{-ik^0(x^0-y^0)}}{(k^0)^2 - \vec{k}^2 - m^2 + i\epsilon} \\ &= -\frac{i}{(2\pi)^3} \int \frac{d^3k}{2k^0} e^{i\vec{k}(\vec{x}-\vec{y}) - ik^0(x^0-y^0)} \Big|_{k^0=\sqrt{\vec{k}^2+m^2}} \cdot \Theta(x^0 - y^0) \\ &\quad - \frac{i}{(2\pi)^3} \int \frac{d^3k}{2k^0} e^{i\vec{k}(\vec{x}-\vec{y}) + ik^0(x^0-y^0)} \Big|_{k^0=\sqrt{\vec{k}^2+m^2}} \cdot \Theta(y^0 - x^0) \end{aligned}$$

which can be written in the following way:

$$iD(x-y) = \frac{1}{(2\pi)^3} \int \frac{d^3k}{2k^0} \left[ e^{-ik(x-y)} \Theta(x^0 - y^0) + e^{ik(x-y)} \Theta(y^0 - x^0) \right]_{k^0=\sqrt{\vec{k}^2+m^2}}. \quad (\text{B.3})$$

This is identical to (B.2) when the Fourier representation (14) for  $\phi$  is inserted. Hence one has the identity

$$\langle 0|T\phi(x)\phi^\dagger(y)|0\rangle = iD(x-y), \quad (\text{B.4})$$

which connects the Green function of the Klein–Gordon equation with the 2-point function of the quantized scalar field and thus with the particle/antiparticle concept obeying causality. As a byproduct, it also explains the extra factor  $i$  in the propagator (19).

## C Loop integrals and dimensional regularization

In the calculation of self-energy diagrams the following type of loop integrals involving two propagators appears when the integration is done in  $D$  dimensions, denoted by  $B_0$  after removing a numerical factor:

$$\mu^{4-D} \int \frac{d^D k}{(2\pi)^D} \frac{1}{[k^2 - m_1^2 + i\varepsilon][(k+q)^2 - m_2^2 + i\varepsilon]} = \frac{i}{16\pi^2} B_0(q^2, m_1, m_2). \quad (\text{C.1})$$

With help of the Feynman parametrization

$$\frac{1}{ab} = \int_0^1 dx \frac{1}{[ax + b(1-x)]^2} \quad (\text{C.2})$$

and after a shift in the  $k$ -variable,  $B_0$  can be written in the form

$$\frac{i}{16\pi^2} B_0(q^2, m_1, m_2) = \int_0^1 dx \frac{\mu^{4-D}}{(2\pi)^D} \int \frac{d^D k}{[k^2 - x^2 q^2 + x(q^2 + m_1^2 - m_2^2) - m_1^2 + i\varepsilon]^2}. \quad (\text{C.3})$$

The advantage of this parametrization is a simpler  $k$ -integration where the integrand is only a function of  $k^2 = (k^0)^2 - \vec{k}^2$ . In order to transform it into a Euclidean integral we perform the substitution <sup>2</sup>

$$k^0 = i k_E^0, \quad \vec{k} = \vec{k}_E, \quad d^D k = i d^D k_E \quad (\text{C.4})$$

where the new integration momentum  $k_E$  has a positive-definite metric:

$$k^2 = -k_E^2, \quad k_E^2 = (k_E^0)^2 + \dots + (k_E^{D-1})^2. \quad (\text{C.5})$$

This leads us to a Euclidean integral over  $k_E$ ,

$$\frac{i}{16\pi^2} B_0 = i \int_0^1 dx \frac{\mu^{4-D}}{(2\pi)^D} \int \frac{d^D k_E}{(k_E^2 + Q)^2} \quad (\text{C.6})$$

where

$$Q = x^2 q^2 - x(q^2 + m_1^2 - m_2^2) + m_1^2 - i\varepsilon \quad (\text{C.7})$$

is a constant with respect to the  $k_E$ -integration. This  $k_E$ -integral is of the general type

$$\int \frac{d^D k_E}{(k_E^2 + Q)^n}$$

of rotational-invariant integrals in a  $D$ -dimensional Euclidean space. They can be evaluated using  $D$ -dimensional polar coordinates (with the substitution  $k_E^2 = R$ ),

$$\int \frac{d^D k_E}{(k_E^2 + Q)^n} = \frac{1}{2} \int d\Omega_D \int_0^\infty dR R^{\frac{D}{2}-1} \frac{1}{(R + Q)^n},$$

yielding

$$\frac{\mu^{4-D}}{(2\pi)^D} \int \frac{d^D k_E}{(k_E^2 + Q)^n} = \frac{\mu^{4-D}}{(4\pi)^{D/2}} \cdot \frac{\Gamma(n - \frac{D}{2})}{\Gamma(n)} \cdot Q^{-n + \frac{D}{2}}. \quad (\text{C.8})$$

The singularities of the initially 4-dimensional integrals are now recovered as poles of the  $\Gamma$ -function for  $D = 4$  and values  $n \leq 2$ .

<sup>2</sup>The  $i\varepsilon$ -prescription in the masses ensures that this is compatible with the pole structure of the integrand.

Although the l.h.s. of (C.8) as a  $D$ -dimensional integral is sensible only for integer values of  $D$ , the r.h.s. has an analytic continuation in the variable  $D$ : it is well defined for all complex values  $D$  with  $n - \frac{D}{2} \neq 0, -1, -2, \dots$ , in particular for

$$D = 4 - \epsilon \quad \text{with } \epsilon > 0. \quad (\text{C.9})$$

For physical reasons we are interested in the vicinity of  $D = 4$ . Hence we consider the limiting case  $\epsilon \rightarrow 0$  and perform an expansion around  $D = 4$  in powers of  $\epsilon$ . For this task we need the following properties of the  $\Gamma$ -function at  $x \rightarrow 0$ :

$$\begin{aligned} \Gamma(x) &= \frac{1}{x} - \gamma + \mathcal{O}(x), \\ \Gamma(-1+x) &= -\frac{1}{x} + \gamma - 1 + \mathcal{O}(x), \end{aligned} \quad (\text{C.10})$$

with Euler's constant

$$\gamma = -\Gamma'(1) = 0.577\dots \quad (\text{C.11})$$

For the integral  $B_0$  we evaluate the integrand of the  $x$ -integration in (C.3) with help of (C.8) as follows:

$$\begin{aligned} \frac{\mu^\epsilon}{(4\pi)^{2-\epsilon/2}} \cdot \frac{\Gamma(\frac{\epsilon}{2})}{\Gamma(2)} \cdot Q^{-\epsilon/2} &= \frac{1}{16\pi^2} \left( \frac{2}{\epsilon} - \gamma + \log 4\pi - \log \frac{Q}{\mu^2} \right) + \mathcal{O}(\epsilon) \\ &= \frac{1}{16\pi^2} \left( \Delta - \log \frac{Q}{\mu^2} \right) + \mathcal{O}(\epsilon). \end{aligned} \quad (\text{C.12})$$

Since the  $\mathcal{O}(\epsilon)$  terms vanish in the limit  $\epsilon \rightarrow 0$  we can skip them in the following. Insertion into (C.3) with  $Q$  from (C.7) yields

$$B_0(q^2, m_1, m_2) = \Delta - \int_0^1 dx \log \frac{x^2 q^2 - x(q^2 + m_1^2 - m_2^2) + m_1^2 - i\varepsilon}{\mu^2}. \quad (\text{C.13})$$

The remaining integration is elementary and the result can be expressed in terms of logarithms. The explicit analytic formula can be found, for example, in Ref. [10].

In the expression (C.12) above we have introduced the abbreviation

$$\Delta = \frac{2}{\epsilon} - \gamma + \log 4\pi \quad (\text{C.14})$$

for the pole singularity combined with the two purely numerical terms that always go together in dimensional regularization. In the  $\overline{MS}$  renormalization scheme, the counter terms required for renormalization cancel just these  $\Delta$  terms appearing in the calculation of amplitudes at the loop level.

## References

- [1] D. Gross and F. Wilczek, *Phys. Rev. Lett.* **30** (1973) 1343; *Phys. Rev.* **D8** (1973) 3633;  
H.D. Politzer, *Phys. Rev. Lett.* **30** (1973) 1346;  
H. Fritzsche, M. Gell-Mann and H. Leutwyler, *Phys. Lett.* **B47** (1973) 365;  
H. Fritzsche and M. Gell-Mann, Current algebra: quarks and what else?, in *16th Int. Conference on High-Energy Physics*, Chicago, 1972, Eds. J. D. Jackson, A. Roberts, and R. Donaldson (National Accelerator Laboratory, Batavia, IL, 1973), p. 135 [arXiv:hep-ph/0208010].
- [2] S.L. Glashow, *Nucl. Phys.* **B22** (1961) 579;  
S. Weinberg, *Phys. Rev. Lett.* **19** (1967) 1264;  
A. Salam, in *Proceedings of the 8th Nobel Symposium*, Ed. N. Svartholm (Almqvist and Wiksell, Stockholm, 1968).

- [3] S.L. Glashow, I. Iliopoulos and L. Maiani, *Phys. Rev.* **D2** (1970) 1285.
- [4] N. Cabibbo, *Phys. Rev. Lett.* **10** (1963) 531;  
M. Kobayashi and K. Maskawa, *Prog. Theor. Phys.* **49** (1973) 652 .
- [5] F. Halzen and A.D. Martin, *Quarks and Leptons: An Introductory Course in Modern Particle Physics* (Wiley, New York, 1984);  
M.E. Peskin and D.V. Schroeder, *An Introduction to Quantum Field Theory* (Addison-Wesley, Reading, MA, 1995);  
A. Denner, M. Böhm and H. Joos, *Gauge Theories of the Strong and Electroweak Interactions* (B.G. Teubner, Stuttgart/Leipzig/Wiesbaden, 2001).
- [6] G. Salam, *A primer on QCD for hadron colliders*, these proceedings.
- [7] M. Lindner, *Lectures on Neutrino Physics*, lectures at this school.
- [8] C. Amsler *et al.* [Particle Data Group], *Phys. Lett.* **B667** (2008) 1.
- [9] G. 't Hooft, *Nucl. Phys.* **B61** (1973) 455;  
W.A. Bardeen, A.J. Buras, D.W. Duke and T. Muta, *Phys. Rev.* **D18** (1978) 3998.
- [10] M. Böhm, W. Hollik and H. Spiesberger, *Fortschr. Phys.* **34** (1986) 687;  
W. Hollik, *Fortschr. Phys.* **38** (1990) 165;  
A. Denner, *Fortschr. Phys.* **41** (1993) 307; Techniques for the calculation of electroweak radiative corrections at the one-loop level and results for W-physics at LEP200, arXiv:hep-ph/07091075.
- [11] F. Jegerlehner, *J. Phys.* **G29** (2003) 101;  
<http://www-com.physik.hu-berlin.de/~fjeger/hadr5n09.f>;  
H. Burkhardt and B. Pietrzyk, *Phys. Rev.* **D72** (2005) 057501.
- [12] T. Teubner, K. Hagiwara, R. Liao, A.D. Martin and D. Nomura, *Update of  $g-2$  of the muon and  $\Delta\alpha$* , arXiv:1001.5401 [hep-ph].
- [13] D. Bardin *et al.*, *Electroweak Working Group Report*, arXiv:hep-ph/9709229;  
*Reports of the Working Group on Precision Calculations for the Z Resonance*, Eds. D. Bardin, W. Hollik and G. Passarino, CERN 95-03 (1995).
- [14] A. Freitas, W. Hollik, W. Walter and G. Weiglein, *Phys. Lett.* **B495** (2000) 338; *Nucl. Phys.* **B632** (2002) 189;  
M. Awramik and M. Czakon, *Phys. Rev. Lett.* **89** (2002) 241801; *Phys. Lett.* **568** (2003) 48;  
A. Onishchenko and O. Veretin, *Phys. Lett.* **B551** (2003) 111;  
M. Awramik, M. Czakon, A. Onishchenko and O. Veretin, *Phys. Rev.* **D68** (2003) 053004.
- [15] J. van der Bij, K. Chetyrkin, M. Faisst, G. Jikia and T. Seidensticker, *Phys. Lett.* **B498** (2001) 156;  
M. Faisst, J. Kühn, T. Seidensticker and O. Veretin, *Nucl. Phys.* **B665** (2003) 649;  
Y. Schroder and M. Steinhauser, *Phys. Lett.* **B622** (2005) 124;  
K. Chetyrkin, M. Faisst, J. Kühn and P. Maierhofer, *Phys. Rev. Lett.* **97** (2006) 102003;  
R. Boughezal and M. Czakon, *Nucl. Phys.* **B755** (2006) 221;  
R. Boughezal, J.B. Tausk and J.J. van der Bij, *Nucl. Phys.* **B725** (2005) 3; **B713** (2005) 278.
- [16] The LEP Collaborations, the LEP Electroweak Working Group, the Tevatron Electroweak Working Group, the SLD Electroweak and Heavy Flavour Working Groups, Precision electroweak measurements and constraints on the Standard Model, CERN-PH-EP/2009-023;  
<http://www.cern.ch/LEPEWWG>.
- [17] M. Awramik, M. Czakon, A. Freitas and G. Weiglein, *Phys. Rev. Lett.* **93** (2004) 201805;  
M. Awramik, M. Czakon and A. Freitas, *Phys. Lett.* **B642** (2006) 563; *JHEP* **0611** (2006) 048;  
W. Hollik, U. Meier and S. Uccirati, *Nucl. Phys.* **B731** (2005) 213; *Phys. Lett.* **B632** (2006) 680;  
*Nucl. Phys.* **B765** (2007) 154.
- [18] H.N. Brown *et al.*, *Phys. Rev. Lett.* **86** (2001) 2227;  
G.W. Bennett *et al.*, *Phys. Rev. Lett.* **89** (2002) 101804; *Phys. Rev. Lett.* **92** (2004) 161802.
- [19] F. Jegerlehner, *Springer Tracts in Modern Physics* **226** (2007);

- F. Jegerlehner and A. Nyffeler, *Phys. Rep.* **477** (2009) 1.
- [20] *LEP2 Monte Carlo Workshop: Report of the Working Groups on Precision Calculations for LEP2 Physics*, Eds. S. Jadach, G. Passarino and R. Pittau, CERN 2000-009 (2000).
- [21] H. Flücher, M. Goebel, J. Haller, A. Höcker, K. Moenig and J. Stelzer, *Eur. Phys. J.* **C60** (2009) 543.
- [22] S. Haywood *et al.*, Electroweak physics, arXiv:hep-ph/0003275, in: *Standard Model Physics (and more) at the LHC*, Eds. G. Altarelli and M. Mangano, CERN 2000-004 (2000), pp. 117–230.
- [23] A. Accomando *et al.*, *Phys. Rep.* **299** (1998) 1;  
J.A. Aguilar-Saavedra *et al.*, *TESLA Technical Design Report, Part 3, Physics at an  $e^+e^-$  Linear Collider*, arXiv:hep-ph/0106315.
- [24] J. Erler, S. Heinemeyer, W. Hollik, G. Weiglein and P.M. Zerwas, *Phys. Lett.* **B486** (2000) 125.
- [25] The TEVNPH Working Group, Combined CDF and D0 upper limits on Standard-Model Higgs-Boson production with 2.1-5.4  $\text{fb}^{-1}$  of data, arXiv:0911.3930 [hep-ex];  
T. Aaltonen *et al.* [CDF and D0 Collaborations], *Phys. Rev. Lett.* **104** (2010) 061802.
- [26] L. Maiani, G. Parisi and R. Petronzio, *Nucl. Phys.* **B136** (1979) 115;  
N. Cabibbo, L. Maiani, G. Parisi and R. Petronzio, *Nucl. Phys.* **B158** (1979) 259;  
R. Dashen and H. Neuberger, *Phys. Rev. Lett.* **50** (1983) 1897;  
D.J.E. Callaway, *Nucl. Phys.* **B233** (1984) 189;  
M.A. Beg, C. Panagiotakopoulos and A. Sirlin, *Phys. Rev. Lett.* **52** (1984) 883;  
M. Lindner, *Z. Phys.* **C31** (1986) 295.
- [27] M. Lindner, M. Sher and H. Zaglauer, *Phys. Lett.* **B228** (1989) 139;  
G. Altarelli and G. Isidori, *Phys. Lett.* **B337** (1994) 141;  
J.A. Casas, J.R. Espinosa and M. Quiros, *Phys. Lett.* **B342** (1995) 171 and **B382** (1996) 374 .
- [28] T. Hambye and K. Riesselmann, *Phys. Rev.* **D55** (1997) 7255.
- [29] J. Kuti, L. Lin and Y. Shen, *Phys. Rev. Lett.* **61** (1988) 678;  
P. Hasenfratz *et al.*, *Nucl. Phys.* **B317** (1989) 81;  
M. Lüscher and P. Weisz, *Nucl. Phys.* **B318** (1989) 705;  
M. Göckeler, H. Kastrup, T. Neuhaus and F. Zimmermann, *Nucl. Phys.* **B404** (1993) 517.
- [30] M. Göckeler, H. Kastrup, J. Westphalen and F. Zimmermann, *Nucl. Phys.* **B425** (1994) 413.
- [31] A. Ghinculov, *Nucl. Phys.* **B455** (1995) 21;  
A. Frink, B. Kniehl and K. Riesselmann, *Phys. Rev.* **D54** (1996) 4548.
- [32] K. Riesselmann, Limitations of a Standard Model Higgs boson, arXiv:hep-ph/9711456.
- [33] T. Binoth, A. Ghinculov and J.J. van der Bij, *Phys. Rev.* **D57** (1998) 1487; *Phys. Lett.* **B417** (1998) 343.
- [34] L. Durand, B.A. Kniehl and K. Riesselmann, *Phys. Rev. Lett.* **72** (1994) 2534 [Erratum-ibid. **74** (1995) 1699];  
A. Ghinculov, *Phys. Lett.* **B337** (1994) 137 [Erratum-ibid. **B346** (1995) 426];  
V. Borodulin and G. Jikia, *Phys. Lett.* **B391** (1997) 434.
- [35] U. Aglietti *et al.*, Tevatron-for-LHC report: Higgs, arXiv:hep-ph/0612172.
- [36] <http://diablo.phys.northwestern.edu/pc/brs.html>
- [37] H.P. Nilles, *Phys. Rep.* **110**, 1 (1984);  
H. Haber and G. Kane, *Phys. Rep.* **117** (1985) 75.
- [38] A. Djouadi, *Phys. Rep.* **459** (2008) 1.
- [39] S. Heinemeyer, W. Hollik and G. Weiglein, *Phys. Lett.* **B440** (1998) 296; *Eur. Phys. J.* **C9** (1999) 343; *Comput. Phys. Commun.* **124** (2000) 76 ;  
G. Degrassi, S. Heinemeyer, W. Hollik, P. Slavich and G. Weiglein, *Eur. Phys. J.* **C28** (2003) 133 ;  
M. Frank, T. Hahn, S. Heinemeyer, W. Hollik, H. Rzehak and G. Weiglein, *JHEP* **0702** (2007) 047;

- T. Hahn, S. Heinemeyer, W. Hollik, H. Rzehak and G. Weiglein, *Comput. Phys. Commun.* **180** (2009) 1426.
- [40] W. Hollik, E. Kraus, M. Roth, C. Rupp, K. Sibold and D. Stöckinger, *Nucl. Phys.* **B639** (2002) 3.
- [41] S. Heinemeyer, W. Hollik and G. Weiglein, *Phys. Rep.* **425** (2006) 265;  
Heinemeyer, W. Hollik, D. Stöckinger, A.M. Weber and G. Weiglein, *JHEP* **0608** (2006) 052;  
Heinemeyer, W. Hollik, A.M. Weber and G. Weiglein, *JHEP* **0804** (2008) 039.
- [42] D. Stöckinger, *J. Phys.* **G34** (2007) 45.
- [43] W. de Boer, A. Dabelstein, W. Hollik and W. Möhle and U. Schwickerath, *Z. Phys.* **C75** (1997) 627;  
W. de Boer and C. Sander, *Phys. Lett.* **B585** (2004) 276.
- [44] O. Buchmueller *et al.*, *Phys. Lett.* **B657** (2007) 87; *JHEP* **0809** (2008) 117.